Table 2. Correlation between Levels of Cox-2 and Laminin-5 Expression in Lung Adenocarcinomas

	Cox-2		
Laminin-5	–	+	2+
–	2	12	4
+	2	42	16
2+	0	13	11

determined by the DC Protein Assay kit (BioRad, Hercules, CA, USA). For Western blotting, equal amounts of protein samples were size-separated on premade 5 to 12.5% gradient polyacrylamide gels (Biocraft, Tokyo, Japan) and electroblotted onto nitrocellulose membranes. Nonspecific binding was blocked by immersion of the membranes for 20 minutes in a solution containing 5% skim milk and 0.1% Tween 20. The membranes were then incubated for 2 hours at room temperature with sheep polyclonal anti-EGFR antibody (at a dilution of ×1/1000; Upstate Biotechnology, Lake Placid, NY), rabbit polyclonal anti-c-erbB-2 antibody (at a concentration of 0.025 μg/ml; Nichirei), rabbit polyclonal anti-ERK1/2 (p42/44 MAP kinase) antibody (at a dilution of ×1/1000; New England Biolabs, Beverly, MA), or rabbit polyclonal phospho-ERK1/2 (Thr202/Tyr204) antibody (at a dilution of ×1/1000; QCB, Camarillo, CA). After washing, the membranes were incubated for 1 hour at room temperature with peroxidase-linked secondary antibody. The antigen was detected using enhanced chemiluminescence Western blotting detection reagents (Amersham, Arlington Heights, IL) following the manufacturer's instructions.

Cell Migration Assay

Cell migration assay was performed using Biocoat cell culture inserts with 8-μm porosity polyethylene teraphthalate filters (BD Biosciences, NJ). Briefly, confluent tumor cells were trypsinized and plated onto the upper chamber and allowed to attach to the membrane for 1 hour. Then TGF-α (50 ng/ml) was added into both upper and lower chambers with or without 50 μmol/L PD98059 (Calbiochem, Darmstadt, Germany) or 100 μmol/L NS-398 (Cayman Chemical, Ann Arbor, MI). Preliminary experiments showed that no cytotoxicity occurred at these concentrations as inspected under the microscope or by the trypan blue exclusion test. Control culture received only vehicle (0.2% dimethyl sulfoxide). Cells were allowed to migrate for 24 hours (A549 cells) or 48 hours (ABC-1 cells). Then, the upper surface of the membrane was wiped to remove nonmigratory cells. Cells that had migrated to the undersurface of the membrane were fixed with methanol, stained with Giemsa solution, and counted. To determine the number of migrated cells for individual wells, cells in five randomly chosen fields were viewed at ×400 magnification with an eyepiece equipped with a grid square, and the number of cells within the largest square was counted, and the means were calculated. The results for each culture condition were expressed as mean ± SE of four individual wells.

Statistics

The correlation between cox-2 and laminin-5 expression was determined by Spearman's rank coefficient. The differences in cox-2 and laminin-5 expression according to the presence or absence of p53 abnormalities or EGFR/erbB-2 overexpression were examined by the Mann-Whitney *U* test. The results were considered significant if the *P* value was <0.05. All tests were two-sided. With regard to the induction of mRNA levels of cox-2 and laminin-5 γ2 by TGF-α in cultured cells, the ratios of TGF-α-treated levels *versus* control levels were calculated for each time point, and the results are expressed as mean ± SE. The differences were considered significant if 1.0 did not lie within the 95% confidence interval of the treated-to-control ratio. Statistical calculations were performed with the StatView computer program (Abacus Concepts, Berkeley, CA).

Results

Co-Localization of Cox-2 and Laminin-5

During the course of our studies on lung cancer, we found that cox-2 was often expressed at the cancer-stromal interface in small-sized lung adenocarcinoma. Because this pattern of expression was similar to that of the laminin-5 γ2 chain,[34] we examined a series of small-sized lung adenocarcinomas for the expression of cox-2 and laminin-5. Overall, cox-2 was expressed in 97 of 102 cases (95.1%), and laminin-5 in 82 of 102 cases (80.3%). Cox-2 and laminin-5 were frequently co-localized in the cytoplasm of cancer cells at the cancer-stromal interface or at the invasive front of the tumors (Figure 1, A and B). Strong staining was typically observed in cancer cells that invaded the fibrous stroma in a scattered manner. In some cases, tumor cells near the necrotic area stained positive for both laminin-5 and cox-2[23] (Figure 1, C and D). A comparison of cox-2 and laminin-5 staining revealed a striking similarity in the distribution of these two proteins in 24 of 102 cases, and a partial overlap between their distribution in another 20 cases. In the remaining cases, discrepancies in distribution occurred owing to a somewhat diffuse staining pattern of cox-2, and to relatively strong cox-2 staining in some bronchioloalveolar carcinomas (Figure 1, E and F) or in some cancer cells that showed bronchioloalveolar carcinoma-like spread along the alveolar structure. Both cox-2 and laminin-5 were localized mainly within the cytoplasm of cancer cells; however, stromal cells, including fibroblasts, endothelial cells, and macrophages, were occasionally stained for cox-2. The expression levels of cox-2 and laminin-5 were then graded on a scale of 0 to 2+ based on the area that showed the highest expression of these proteins (see Materials and Methods). As shown in Table 2, a positive correlation was found between the expression levels of cox-2 and laminin-5 ($P = 0.018$).

Table 3. Summary of 58 Cases of Stage I Lung Adenocarcinoma

Case	Age	Sex	Size	WHO	Diff.	Laminin-5	Cox-2	EGFR	ErbB-2	p53 IHC	p53 Mutation	Exon	Codon	Nucleotide change	Amino acid change
N141T	64	M	7	pap	M	1+	2+	−	+	+	+	5	141	TGC to TAC	Lys to Tyr
A011T	67	M	4.3	mix	W	2+	1+	−	+	+	+	6	220	TAT to TGT	Tyr to Cys
Q181T	69	M	2.7	sol	P	2+	2+	+	+	+	+	7	242	CTT to CGT	Leu to Arg
Q311T	63	M	2.5	mix	M	1+	1+	−	+	+	+	8	283	CGC to CCC	Arg to Pro
Q491T	59	F	4.6	aci	M	2+	1+	−	−	+	+	6	194	CTT to CGT	Leu to Arg
Q191T	56	M	3.3	mix	M	2+	2+	+	−	+	+	7	250	CCC to CTC	Pro to Leu
Q691T	45	F	1.8	mix	W	1+	1+	−	−	+	+	5	157	GTC to TTC	Val to Phe
												5	143	GTG to xTG	frameshift
Q701T	57	M	2.5	sol	P	2+	2+	+	−	+	+	5	158	CGC to CTC	Arg to Leu
Q721T	49	M	2.2	mix	W	1+	2+	+	+	+	+	8	281	GAC to CAC	Asp to His
Q771T	60	M	1.9	mix	W	−	1+	−	−	+	+	8	282	CGG to TGG	Arg to Trp
Q861T	49	F	1.9	mix	W	1+	2+	+	−	+	+	6	213	CGA to CAA	Arg to Gln
Q591T	66	M	16	mix	W	2+	2+	−	−	+	+	7	247	AAC to ATC	Asn to Ile
Q391T	72	M	2	pap	M	2+	1+	−	+	−	+	8	298	GAG to TAG	Glu to stop
Q351T	73	F	3.5	mix	W	1+	2+	+	+	−	+	4	64	CCC to xCC	frameshift
Q801T	72	M	5.5	mix	M	2+	2+	+	+	−	+	9	317	CAG to xAG	frameshift
Q121T	56	M	3.1	mix	M	2+	2+	+	+	+	−				
Q571T	64	M	4	pap	M	2+	1+	+	+	+	−				
Q551T	52	F	1.6	pap	M	2+	2+	−	−	+	−				
Q411T	67	M	5	sol	P	2+	2+	+	−	+	−				
Q461T	66	F	2.9	pap	M	2+	1+	+	+	+	−				
Q511T	76	M	2.5	mix	W	1+	1+	−	−	+	−				
Q611T	55	F	2.5	mix	W	2+	2+	+	+	+	−				
Q621T	65	M	2.5	mix	W	2+	2+	+	+	+	−				
Q761T	72	F	2.8	mix	W	1+	−	−	−	+	−				
1041T	38	F	7	pap	M	2+	1+	−	−	−	−				
1151T	57	F	3.3	mix	W	1+	1+	−	+	−	−				
2071T	55	M	2.5	mix	W	−	−	−	−	−	−				
Q131T	60	M	5.4	aci	M	2+	2+	−	−	−	−				
Q151T	70	M	7	mix	M	1+	2+	+	+	−	−				
Q141T	75	M	3.8	aci	W	2+	1+	−	+	−	−				
Q171T	79	M	3.7	sol	P	2+	2+	−	−	−	−				
Q561T	62	M	2.2	mix	W	1+	1+	−	−	−	−			(Polymorphism)	
Q421T	50	F	1.6	pap	M	1+	1+	−	−	−	−				
Q291T	71	F	2	bac	W	1+	1+	−	−	−	−				
Q321T	62	M	2.2	mix	M	2+	2+	−	−	−	−				
Q261T	63	M	3.2	mix	W	2+	2+	−	−	−	−				
Q251T	67	M	3.8	mix	W	1+	1+	−	+	−	−			(Silent)	
Q281T	59	F	2.6	mix	W	1+	−	−	−	−	−			(Silent)	
Q361T	52	M	4	bac	W	−	1+	−	−	−	−				
Q371T	65	F	1.3	mix	M	1+	1+	−	−	−	−				
Q301T	59	F	1.9	mix	W	1+	2+	−	−	−	−				
Q381T	50	F	1.9	pap	M	2+	2+	−	+	−	−				
Q451T	73	F	4	mix	W	2+	1+	−	+	−	−				
Q501T	78	F	3.2	mix	M	2+	1+	−	+	−	−				
Q481T	58	F	2.5	mix	W	1+	1+	−	−	−	−				
Q441T	55	F	2.3	mix	M	1+	1+	−	−	−	−				
Q631T	57	M	2.5	mix	M	1+	1+	−	−	−	−				
Q651T	63	M	3.5	mix	W	1+	1+	−	−	−	−				
Q661T	70	M	2.1	pap	M	2+	2+	+	−	−	−				
Q671T	55	F	3.2	mix	W	1+	1+	+	−	−	−				
Q581T	73	M	3.8	aci	W	1+	2+	+	−	−	−				
Q821T	54	M	3.2	mix	W	1+	1+	+	−	−	−				
Q841T	57	M	2.4	mix	M	1+	1+	−	−	−	−				
Q851T	70	F	3.2	mix	W	1+	1+	−	−	−	−				
Q911T	65	M	2.8	aci	M	2+	2+	+	+	−	−				
Q931T	65	M	2.5	sol	P	2+	2+	+	−	−	−				
Q941T	74	M	2.8	pap	M	1+	−	−	−	−	−				
Q951T	62	M	2.7	sol	P	2+	−	+	+	−	−				
Q961T	71	M	3.8	mix	P	2+	2+	+	+	−	−				

WHO, World Health Organization histological classification; pap, papillary adenocarcinoma; aci, acinar adenocarcinoma; sol, solid adenocarcinoma with mucin; mix, adenocarcinoma with mixed subtypes; Diff, differentiation; W, well; M, moderately; P, poorly differentiated.

P53 IHC, p53 overexpression by immunohistochemistry. X in nucleotide change indicates one base deletion. Q691T had two distinct p53 mutations. Q561T had a nucleotide change that was interpreted as a polymorphism. Q251T and Q281T, which had a silent mutation, were included in the group negative for p53 mutation.

Table 4. Expression Levels of Cox-2 and Laminin-5 According to the Presence or Absence of p53 Mutation or Overexpression

		Cox-2			Laminin-5		
		−	+	2+	−	+	2+
A							
p53 mutation	−	5	22	16	3	20	20
	+	0	6	9	0	7	8
				$P = 0.0802$			$P = 0.5153$
B		Cox-2			Laminin-5		
		−	+	2+	−	+	2+
p53 overexpression	−	5	20	13	3	20	15
	+	0	8	12	0	7	13
				$P = 0.0316$			$P = 0.0474$

Relationships of p53 Status with Expression of Cox-2 and Laminin-5

The genetic mechanisms underlying the overexpression of cox-2 and laminin-5 in cancer are not clearly understood. However, a recent study by Subbaramaiah and colleagues[33] suggested a potential role of p53 in suppressing the expression of cox-2. Therefore, we studied the relationships between p53 status and the expression of cox-2 and laminin-5 in 58 cases of stage I lung adenocarcinomas. We determined the p53 status of these cases by PCR-single strand conformation polymorphism analysis and direct sequencing. We also immunohistochemically studied the overexpression of p53. Overall, p53 mutation was found in 15 of 58 cases (25.9%), and p53 overexpression in 20 of 58 cases (34.5%). Data concerning p53 mutation and other immunohistochemical results are shown in Table 3. Three tumors with p53 mutation were negative for p53 overexpression, whereas eight tumors without p53 mutation overexpressed p53. The concordance rate of p53 mutation and overexpression was 81.0%. The relationships between p53 status and the expression of cox-2 and laminin-5 are shown in Table 4. Tumors with mutant p53 showed a tendency for higher expression levels of cox-2 than those with wild-type p53 ($P = 0.080$) (Table 4A). Also, tumors that overexpressed p53 had higher expression levels of cox-2 and laminin-5 than those without p53 overexpression ($P = 0.032$ and $P = 0.047$, respectively) (Table 4B).

Relationships of EGFR/erbB-2 versus *Cox-2/ Laminin-5 Expression*

Previous *in vitro* studies suggested that cox-2 could be induced by tumor necrosis factor-α,[31] IL-1β,[29,30] and EGFR signaling,[27,28] whereas the expression of laminin-5 could be stimulated by epidermal growth factor (EGF) and phorbol myristate acetate.[52] Because EGFR seemed to be a common upstream regulator of cox-2 and laminin-5, we immunohistochemically studied the expression of EGFR and its heterodimeric partner erbB-2 in the 58 cases of stage I lung adenocarcinoma. The results showed that the expression levels of cox-2 and laminin-5 were higher in tumors that overexpressed both EGFR and erbB-2 than in those without concomitant overexpression of these proteins ($P = 0.014$ and $P = 0.019$, respectively) (Table 5).

Expression Analyses of Cox-2, Laminin-5, EGFR, and ErbB-2 in Lung Adenocarcinoma Cell Lines

Next, we investigated whether similar relationships occurred in lung adenocarcinoma cell lines. We analyzed six cell lines: A549, HLC-1, ABC-1, LC-2/ad, VMRC-LCD, and L27. The results are shown in Figures 2 and 3. Quantitative RT-PCR analysis showed that three cell lines (ABC-1, LC-2/ad, and L27) expressed mRNAs of cox-2 and laminin-5 γ2 chain at relatively high levels, and that two lines (HLC-1 and VMRC-LCD) expressed them at low levels (Figure 2, A and B). Cell line A549 had a high level of cox-2 mRNA but a low level of laminin-5 γ2 chain mRNA. Western blot analysis showed that both EGFR and erbB-2 were expressed at variable levels in all cell lines except VMRC-LCD (Figure 3, A and B). A comparison between Figures 2 and 3 shows that mRNA levels of cox-2, and to a lesser extent laminin-5 γ2, correlated well not only with erbB-2 but also with the phosphorylated form of MAPK/ERK-1/2 (Figure 3, B and C), one of the major downstream molecules in the EGFR signaling pathway. The levels of total ERK-1/2 were similar in all cell lines examined (Figure 3D).

Table 5. Expression Levels of Cox-2 and Laminin-5 According to the Presence or Absence of Concomitant Overexpression of EGFR and ErbB-2

Overexpression of EGFR and erbB-2	Cox-2			Laminin-5		
	−	+	2+	−	+	2+
−	4	26	15	3	24	18
+	1	2	10	0	3	10
			$P = 0.0139$			$P = 0.0180$

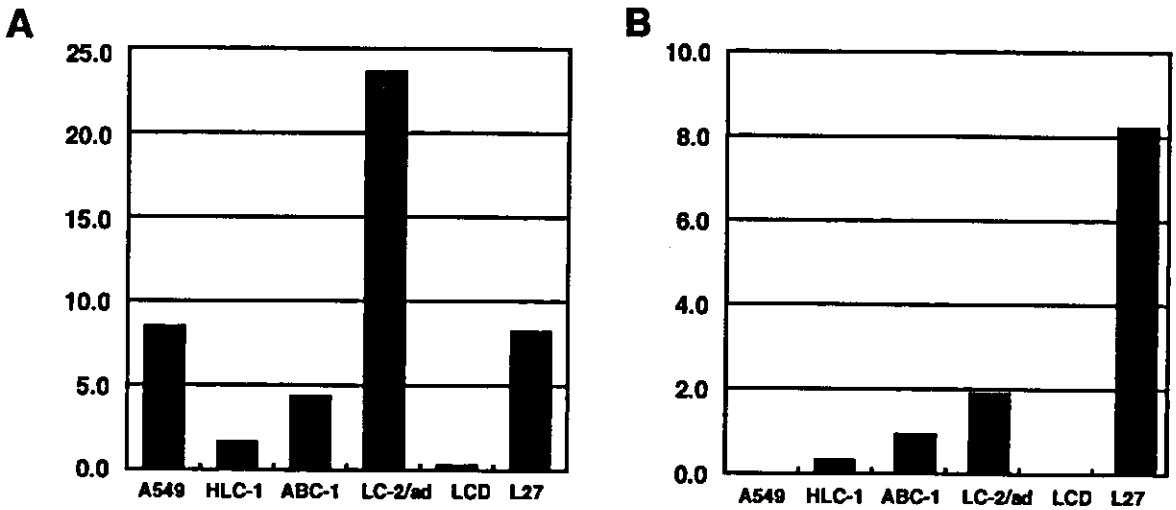

Figure 2. Levels of cox-2 (**A**) and laminin-5 γ2 (**B**) mRNAs in lung adenocarcinoma cell lines. Levels of mRNAs were determined by real-time quantitative RT-PCR analysis. After normalization for 18S rRNA, data were expressed in arbitrary units. The results are the mean of duplicate measurements. Three cell lines (ABC-1, LC-2/ad, and L27) expressed cox-2 and laminin-5 γ2 chain mRNA at relatively high levels. Two lines (HLC-1 and VMRC-LCD) expressed them at low levels. Line A549 had a relatively high level of cox-2 mRNA, but a very low level of laminin-5 γ2 chain mRNA. LCD indicates VMRC-LCD.

Effect of TGF-α on Cox-2 and Laminin-5 γ2 Chain mRNAs

Next, we looked to see whether the addition of TGF-α, one of the ligands for EGFR, could stimulate the expression of cox-2 and laminin-5 γ2 mRNAs. Four cells lines—A549, ABC-1, L27, and LC-2/ad—were exposed to 50 ng/ml of TGF-α for up to 24 hours. Total RNA was isolated at 1, 3, 8, and 24 hours, and subjected to real-time RT-PCR analysis. Results are shown in Figure 4, A and B. Treatment with TGF-α increased cox-2 mRNA levels 2.6-fold in A549, 11.4-fold in ABC-1, and 1.8-fold in L27. Laminin-5 γ2 mRNA levels were also stimulated 3.2-fold in A549, 4.1-fold in ABC-1, and 1.4-fold in L27. A comparison of Figure 4, A and B, shows that the induction kinetics differed for cox-2 and laminin-5; cox-2 mRNA levels peaked early at 1 hour, whereas laminin-5 γ2 was induced gradually for up to 24 hours. Treatment with TGF-α did not induce any significant change in mRNA levels of cox-2 or laminin-5 γ2 chain in LC-2/ad (data not shown).

Expression of Laminin-5 α3, β3, and γ2 Chains in Lung Adenocarcinomas

Although the induction of laminin-5 at the invasive front is consistent with the hypothesis that laminin-5 contributes to the invasion of cancer cells, the predominantly cytoplasmic localization of laminin-5 γ2 chain raises some doubt as to whether laminin-5 is ever secreted and deposited as an extracellular matrix, and whether our laminin-5 γ2 chain antibody may not recognize matrix-deposited form of laminin-5. Also, Koshikawa and colleagues[42] recently reported that laminin-5 γ2 chain was strongly expressed at the invasive margin of cancer cells without detectable signal for laminin-5 β3 or α3. To address these issues, we used commercially available antibodies against laminin α3, β3, and γ2 chains, and compared the staining patterns of these antibodies to those of our laminin-5 γ2 antibody. Thus, in total, we tested six antibodies, ie, two antibodies for each chain of laminin-5. The results are shown in Figure 5; A to C. Laminin α3 chain was weakly positive in most cases of lung adenocarcinoma cells. In comparison to laminin γ2 chain, however, the staining pattern of α3 chain was diffuse and localization at the invasive front was not evident in most cases. Poorly differentiated adenocarcinomas tended to be negative for laminin α3 chain. In contrast, laminin β3 chain showed a staining pattern identical to that of γ2 chain. Although laminin-5 γ2 chain was mainly localized in the cytoplasm of invading cancer cells, we did observe staining of basement membrane for laminin γ2 chain, especially when 3,3′-diaminobenzidine tetrahydrochloride reaction was extended (Figure 5, D and E). These results were the same for each pair of antibodies.

The Effect of Cox-2 and MAPK Kinase Inhibitors on Tumor Cell Migration

Finally, we investigated the roles of MAPK kinase cascade and cox-2 in tumor cell migration that occur after stimulation with TGF-α. For this purpose we used a pharmacological inhibitor of MAPK kinase, PD98059, and a selective cox-2 inhibitor, NS-398. The results are shown in Figure 6. In ABC-1 cells, both PD98059 and NS-398 strongly inhibited cell migration. In contrast, A549 cells showed different responses to these inhibitors; PD98059 strongly inhibited the migration of A549 cells, but NS-398 was much less effective.

Discussion

We have shown that cox-2 and laminin-5 γ2 chain are frequently co-localized at the cancer-stromal interface and at the invasive front of tumors. We often observed

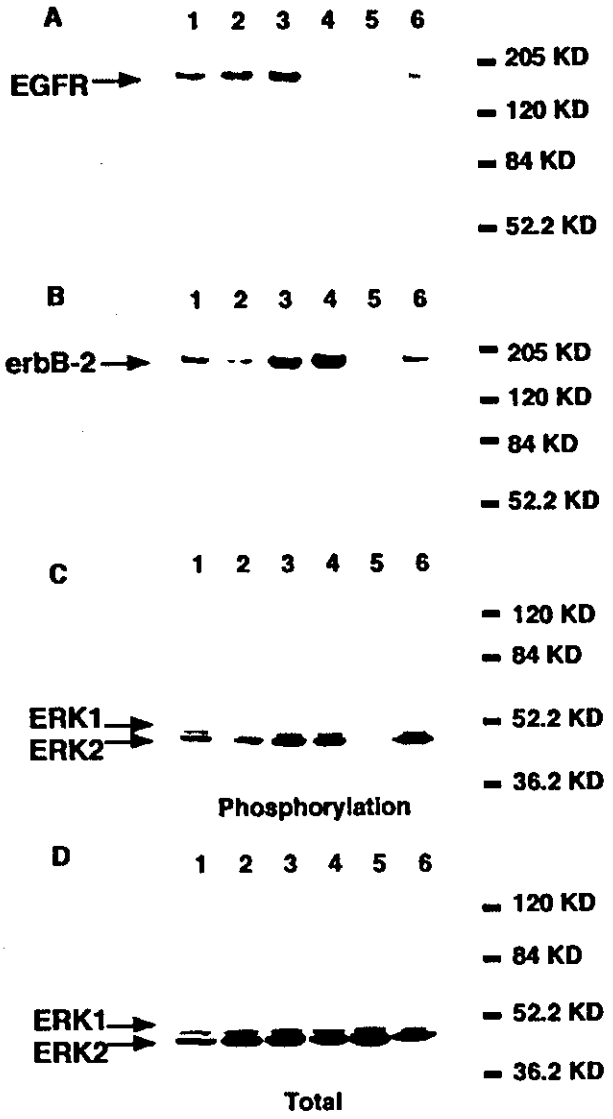

Figure 3. Expression of EGFR (**A**), erbB-2 (**B**), phosphorylated form of ERK-1/2 (**C**), and total ERK-1/2 protein (**D**) in lung adenocarcinoma cell lines (Western blotting). **Lane 1**, A549; **lane 2**, HLC-1; **lane 3**, ABC-1; **lane 4**, LC-2/ad; **lane 5**, VMRC-LCD; **lane 6**, L27. Both EGFR and erbB-2 were expressed at variable levels in all cell lines except VMRD-LCD (**A** and **B**). mRNA levels of cox-2 and to a lesser extent laminin-5 γ2 correlated well not only with erbB-2 but also with the phosphorylated form of MAPK/ERK-1/2 (**B** and **C**; see Figure 2). The levels of total ERK-1/2 were similar in all cell lines examined (**D**).

strong expression of these two proteins in cancer cells that invaded the fibrous stroma in a scattered manner. Expression levels of these proteins were also strongly correlated. In recent years, cox-2 has been the subject of intensive investigation in cancer research. Those studies collectively suggest that cox-2 plays an important role in carcinogenesis, tumor angiogenesis, and metastasis of colon cancer.[1–4] Cox-2 is frequently overexpressed in various types of cancer, including lung cancer.[17–25] It has been shown that high levels of cox-2 protein expression correlate with poor prognosis of patients with stage I lung adenocarcinoma.[25] However, the precise role of cox-2 in the development and progression of cancer is not fully understood. Our results provide a link between cox-2 and laminin-5, a molecule that plays an important role in cell migration and cancer invasion. The frequent co-localization of cox-2 and laminin-5 points to the existence of a mechanism that regulates tumor cell invasion, angiogenesis, and metastasis in a coordinated manner.

Previous *in vitro* studies have shown that the expression of cox-2 is induced by tumor necrosis factor-α,[31] IL-1β,[29,30] and EGFR signaling,[27,28] whereas the expression of laminin-5 can be stimulated by EGF and phorbol myristate acetate.[52] Recent data from our laboratory also show that in squamous cell carcinoma cell lines, the expression levels of laminin-5 correlate with gene amplification of EGFR.[53] Thus, EGFR signaling would be a common upstream regulator of cox-2 and laminin-5. The results of the present study are consistent with this hypothesis; lung adenocarcinomas that overexpressed EGFR and erbB-2, a heterodimeric partner of the EGFR family, had higher levels of cox-2 and laminin-5 than those without concomitant overexpression of these proteins. It has been shown that erbB-2 potentiates EGFR signaling.[54] Also, treatment with TGF-α increased the expression levels of mRNA of cox-2 and laminin-5 γ2 chain.

Although EGFR signaling seems to be involved in the induction of cox-2 and laminin-5, the induction kinetics were different. Also, the magnitude of response to TGF-α was different in different cell lines tested. These observations suggest that the expression of cox-2 and laminin-5 is not regulated in the same manner. Clearly, further investigations are required to elucidate the regulatory mechanisms for the expression of these molecules. In this regard, another candidate molecule likely to be involved in the regulation of cox-2 and laminin-5 is nuclear factor (NF)-κB. NF-κB was initially isolated as a transcription factor regulating immunoglobulin gene expression in B lymphocytes.[55] Studies show that NF-κB plays a key role in inflammation, tissue remodeling, and possibly cancer.[56] NF-κB is involved in the gene regulation of urokinase-type plasminogen activator,[57] vascular endothelial growth factor,[58] and IL-8.[58,59] Indeed, a putative NF-κB binding site, as well as two AP-1 sites, can be identified in the promoter sequence of the human laminin-5 γ2 gene (data not shown). We are currently investigating whether IL-1β and tumor necrosis factor-α stimulate the expression of cox-2 and laminin-5 in a coordinated manner in lung adenocarcinoma cell lines, and if so, whether inhibitors of NF-κB attenuate this stimulating effect.

Another explanation for the co-expression of cox-2 and laminin-5 in lung adenocarcinoma may be that prostaglandins produced through the action of cox-2 up-regulate laminin-5. This hypothesis could be tested by investigating whether the addition of PGE2 or other prostaglandins to culture media stimulates laminin-5 expression in lung adenocarcinoma cell lines.

Previous studies showed that introduction of cox-2 cDNA resulted in a clone of cells expressing high levels of angiogenic factors, including fibroblast growth factors 1 and 2, vascular endothelial growth factor, and platelet-derived growth factor.[15,16] With regard to cell migration, Tsujii and colleagues[16] also showed that cox-2 overexpression in colon cancer cells promoted the motility of

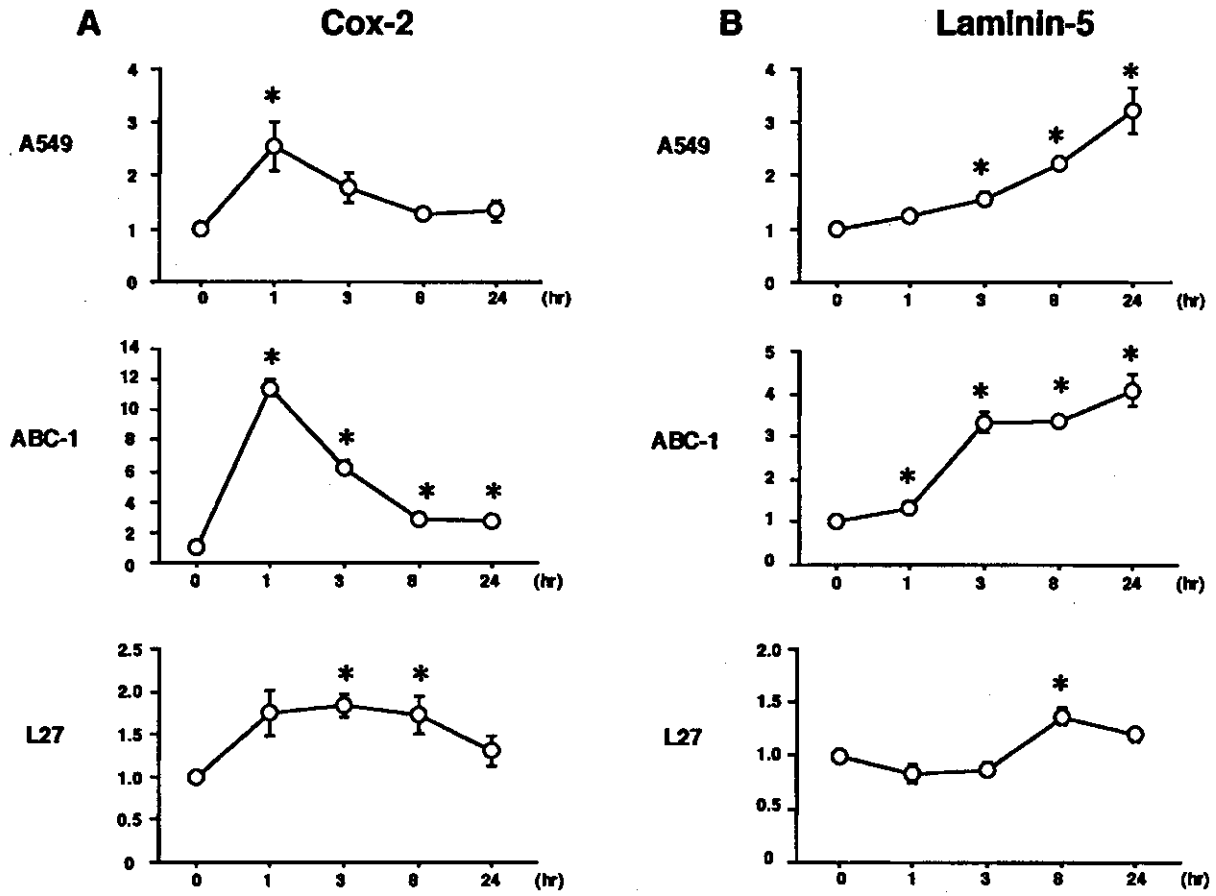

Figure 4. Lung adenocarcinoma cell lines A549, ABC-1, and L27 were exposed to 50 ng/ml of TGF-α for up to 24 hours. Total RNA was isolated at 1, 3, 8, and 24 hours, and subjected to real-time RT-PCR analysis. Treatment with TGF-α increased cox-2 mRNA levels 2.6-fold in A549, 11.4-fold in ABC-1, and 1.8-fold in L27 (**A**). Laminin-5 γ2 mRNA levels were also stimulated 3.2-fold in A549, 4.1-fold in ABC-1, and 1.4-fold in L27 (**B**). Cox-2 mRNA levels peaked early at 1 hour, whereas laminin-5 γ2 was induced gradually for up to 24 hours. Error bars indicate SE of quadruplicate measurements. *, $P < 0.05$.

co-cultured endothelial cells. Several recent studies also indicate that cox-2 is involved in migration of cancer cells,[60–64] consistent with the our results obtained with NS-398. However, our data indicate that the role of cox-2 in cell migration is cell-dependent; cox-2 inhibitor inhibited the migration of ABC-1 cells, but was much less effective toward A549 cells. The basis of such cell-specific effect is unknown, and this issue certainly deserves further investigations. The relative contribution of laminin-5 and cox-2 in cancer cell invasion remains unclear, too. Blocking antibody that specifically inhibits motility-promoting function of laminin-5 would be required to address this issue.

Recently, Koshikawa and colleagues[42] reported that laminin-5 γ2 chain was strongly expressed at the invasive margin of cancer cells without significant signal for laminin-5 β3 or α3. These authors also demonstrated the secretion of the laminin γ2 monomer, as well as the laminin-5 heterotrimer, by two-dimensional sodium dodecyl sulfate-polyacrylamide gel electrophoresis. They speculated that the monomeric form of the γ2 chain may have a function distinct from the laminin-5 trimer. In contrast to their results, we observed identical staining pattern for the laminin β3 and γ2 chains. Sordat and colleagues[41] also found co-expression of the laminin β3 and γ2 chains in colorectal cancers. We do not know the reason for these discrepancies, but it may be because of the use of different antibodies and/or different types of cancer specimens investigated. Certainly, these issues need to be addressed by further investigations.

It has been reported that laminin-5 may perform two opposite functions, ie, promoting cell migration and assembly of hemidesmosomes. Giannelli and colleagues[65] reported that the cleavage of the laminin γ2 chain by MMP-2 elicits cell migration on laminin-5. Conversely, after cleavage of the laminin α3 chain by plasmin, laminin-5 impedes cell motility and promotes hemidesmosome assembly.[66] Thus, different functions of laminin-5 could be explained by differential processing of the subunits that comprise laminin-5. More recently, Koshikawa and colleagues[67] found that MT1-MMP, which cleaves laminin γ2 chain more efficiently than MMP-2, plays essential roles in cell migration on laminin-5. These authors found that cell migration on laminin-5 was significantly reduced by metalloproteinase inhibitors and MT1-MMP antisense oligonucleotides.[67] Interestingly, they found co-localization of MT1-MMP and laminin-5 in breast and colon cancer tissues. Whether cox-2 is directly involved in induction of MMPs[16] and/or processing of laminin-5 needs to be explored in the future.

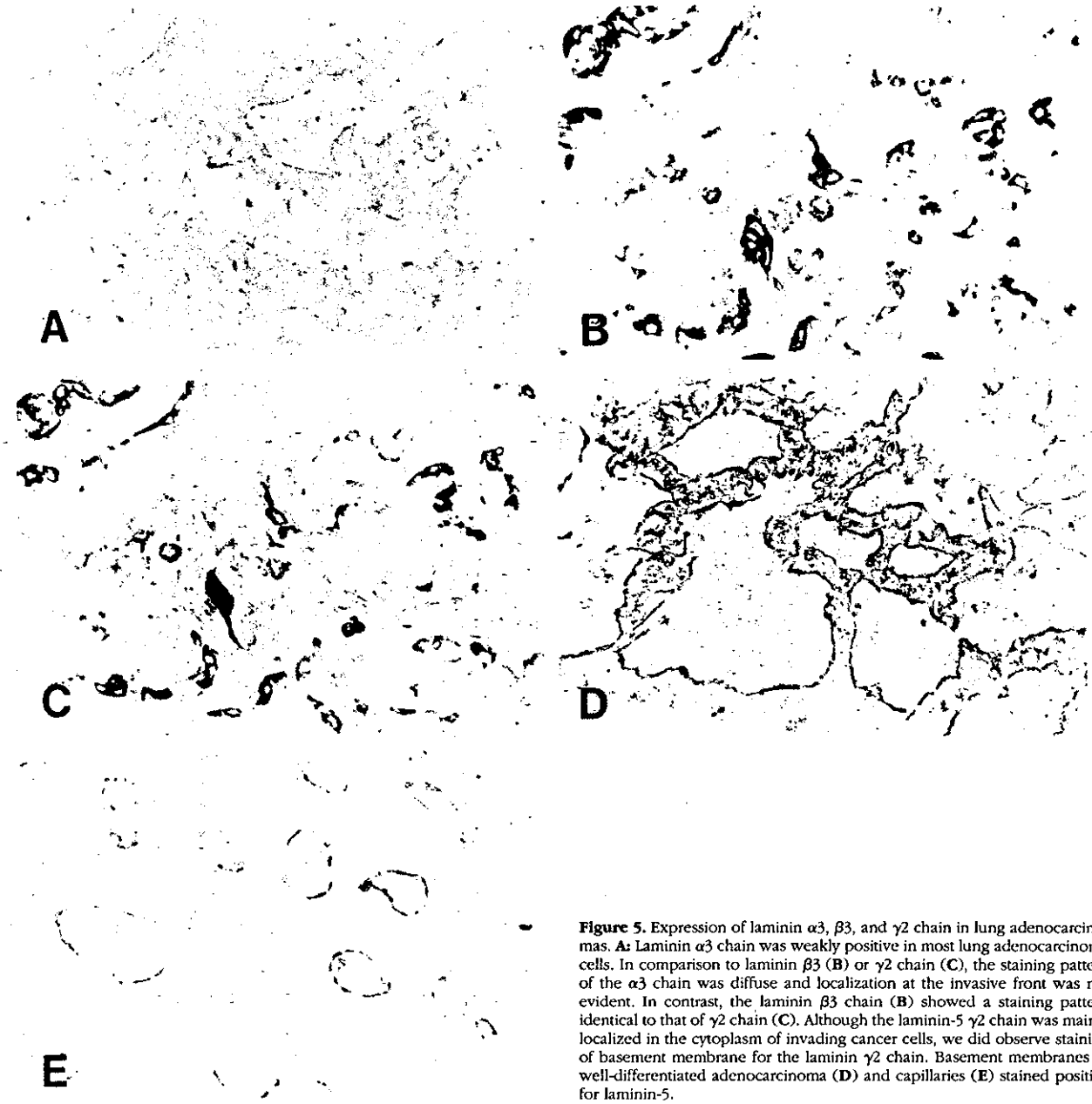

Figure 5. Expression of laminin α3, β3, and γ2 chain in lung adenocarcinomas. **A:** Laminin α3 chain was weakly positive in most lung adenocarcinoma cells. In comparison to laminin β3 (**B**) or γ2 chain (**C**), the staining pattern of the α3 chain was diffuse and localization at the invasive front was not evident. In contrast, the laminin β3 chain (**B**) showed a staining pattern identical to that of γ2 chain (**C**). Although the laminin-5 γ2 chain was mainly localized in the cytoplasm of invading cancer cells, we did observe staining of basement membrane for the laminin γ2 chain. Basement membranes of well-differentiated adenocarcinoma (**D**) and capillaries (**E**) stained positive for laminin-5.

With regard to the negative regulation of cox-2 and laminin-5, it has recently been shown that wild-type p53 suppresses promoter activities of cox-2 and the expression of cox-2 protein.[33] This observation prompted us to examine whether expression levels of cox-2 or laminin-5 are associated with the p53 status of tumor cells. Our results showed that p53 abnormalities, including p53 mutation and overexpression, were associated with overexpression of cox-2 and laminin-5. p53 mutation in tumor cells is associated with poor prognosis of patients in various cancers.[68] The reason for this association is not clear, but it is possible that overexpression of cox-2 or laminin-5 could be at least partially responsible for the poor prognosis of patients with tumors bearing a p53 mutation or overexpression. In this regard, it is noteworthy that wild-type p53 has a suppressive effect on the expression of other genes involved in inflammation and tissue remodeling, including vascular endothelial growth factor,[69] the inducible isoform of nitric oxide synthase,[70] and IL-6.[71]

In summary, we have shown frequent co-localization of cox-2 and laminin-5 at the invasive front of early-stage lung adenocarcinomas, and provided data that support the hypothesis that p53 abnormalities and EGFR signaling are involved in the aberrant expression of these proteins. The data point to the existence of a mechanism that co-regulates the expression of these proteins at the invasive front of cancer, probably facilitating tumor angiogenesis and invasion in a coordinated manner. Further investigations are warranted to elucidate the role of p53 and EGFR signaling in the regulation of cox-2 and laminin-5.

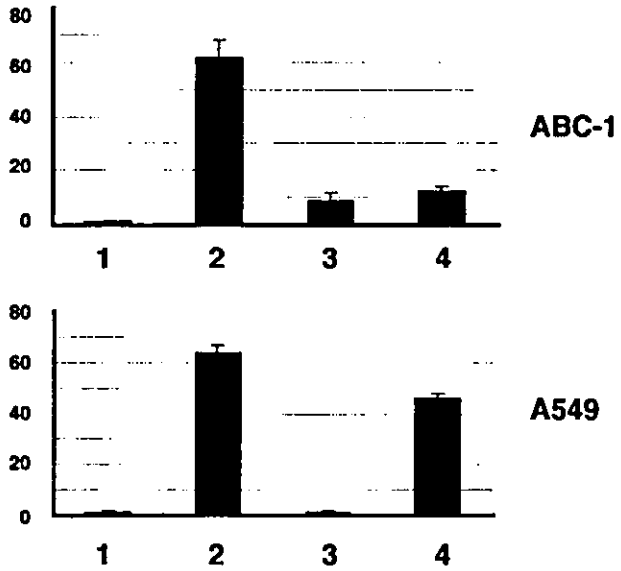

Figure 6. The effect of cox-2 and MAPK kinase inhibitors on migration of lung adenocarcinoma cells. Cell migration assay was performed using cell culture inserts. The number of cells that had migrated to the undersurface of the membranes was counted as stated in Materials and Methods. In ABC-1 cells, both PD98059 (50 μmol/L) and NS-398 (100 μmol/L) strongly inhibited cell migration. In contrast, A549 cells showed different responses to these inhibitors; PD98059 strongly inhibited the migration of A549 cells, but NS-398 was much less effective. 1, control (+0.2% DMSO); 2, TGF-α (50 ng/ml) (+0.2% DMSO); 3, PD98059 (50 μmol/L); 4, NS-398 (100 μmol/L). Results are given as mean ± SE of four wells.

Acknowledgments

We thank Y. Ono, Y. Nakanishi, and Y. Ino for anti-laminin-5 antibody; Y. Yamauchi and A. Harada for technical assistance; and M. Suzuki for secretarial work.

References

1. Taketo MM: Cyclooxygenase-2 inhibitors in tumorigenesis (part I). J Natl Cancer Inst 1998, 90:1529–1536
2. Taketo MM: Cyclooxygenase-2 inhibitors in tumorigenesis (part II). J Natl Cancer Inst 1998, 90:1609–1620
3. Dubois RN, Abramson SB, Crofford L, Gupta RA, Simon LS, Van De Putte LB, Lipsky PE: Cyclooxygenase in biology and disease. FASEB J 1998, 12:1063–1073
4. Williams CS, Mann M, DuBois RN: The role of cyclooxygenases in inflammation, cancer, and development. Oncogene 1999, 18:7908–7916
5. Eberhart CE, Coffey RJ, Radhika A, Giardiello FM, Ferrenbach S, DuBois RN: Up-regulation of cyclooxygenase 2 gene expression in human colorectal adenomas and adenocarcinomas. Gastroenterology 1994, 107:1183–1188
6. Sano H, Kawahito Y, Wilder RL, Hashiramoto A, Mukai S, Asai K, Kimura S, Kato H, Kondo M, Hla T: Expression of cyclooxygenase-1 and -2 in human colorectal cancer. Cancer Res 1995, 55:3785–3789
7. Kargman SL, O'Neill GP, Vickers PJ, Evans JF, Mancini JA, Jothy S: Expression of prostaglandin G/H synthase-1 and -2 protein in human colon cancer. Cancer Res 1995, 55:2556–2559
8. Reddy BS, Hirose Y, Lubet R, Steele V, Kelloff G, Paulson S, Seibert K, Rao CV: Chemoprevention of colon cancer by specific cyclooxygenase-2 inhibitor, celecoxib, administered during different stages of carcinogenesis. Cancer Res 2000, 60:293–297
9. Kawamori T, Rao CV, Seibert K, Reddy BS: Chemopreventive activity of celecoxib, a specific cyclooxygenase-2 inhibitor, against colon carcinogenesis. Cancer Res 1998, 58:409–412
10. Steinbach G, Lynch PM, Phillips RK, Wallace MH, Hawk E, Gordon GB, Wakabayashi N, Saunders B, Shen Y, Fujimura T, Su LK, Levin B: The effect of celecoxib, a cyclooxygenase-2 inhibitor, in familial adenomatous polyposis. N Engl J Med 2000, 342:1946–1952
11. Sheng H, Shao J, Kirkland SC, Isakson P, Coffey RJ, Morrow J, Beauchamp RD, DuBois RN: Inhibition of human colon cancer cell growth by selective inhibition of cyclooxygenase-2. J Clin Invest 1997, 99:2254–2259
12. Liu XH, Yao S, Kirschenbaum A, Levine AC: NS398, a selective cyclooxygenase-2 inhibitor, induces apoptosis and down-regulates bcl-2 expression in LNCaP cells. Cancer Res 1998, 58:4245–4249
13. Elder DJ, Halton DE, Hague A, Paraskeva C: Induction of apoptotic cell death in human colorectal carcinoma cell lines by a cyclooxygenase-2 (COX-2)-selective nonsteroidal anti-inflammatory drug: independence from COX-2 protein expression. Clin Cancer Res 1997, 3:1679–1683
14. Sawaoka H, Kawano S, Tsuji S, Tsujii M, Gunawan ES, Takei Y, Nagano K, Hori M: Cyclooxygenase-2 inhibitors suppress the growth of gastric cancer xenografts via induction of apoptosis in nude mice. Am J Physiol 1998, 274:G1061–G1067
15. Tsujii M, Kawano S, DuBois RN: Cyclooxygenase-2 expression in human colon cancer cells increases metastatic potential. Proc Natl Acad Sci USA 1997, 94:3336–3340
16. Tsujii M, Kawano S, Tsuji S, Sawaoka H, Hori M, DuBois RN: Cyclooxygenase regulates angiogenesis induced by colon cancer cells. Cell 1998, 93:705–716
17. Hwang D, Scollard D, Byrne J, Levine E: Expression of cyclooxygenase-1 and cyclooxygenase-2 in human breast cancer. J Natl Cancer Inst 1998, 90:455–460
18. Ristimaki A, Honkanen N, Jankala H, Sipponen P, Harkonen M: Expression of cyclooxygenase-2 in human gastric carcinoma. Cancer Res 1997, 57:1276–1280
19. Mohammed SI, Knapp DW, Bostwick DG, Foster RS, Khan KN, Masferrer JL, Woerner BM, Snyder PW, Koki AT: Expression of cyclooxygenase-2 (COX-2) in human invasive transitional cell carcinoma (TCC) of the urinary bladder. Cancer Res 1999, 59:5647–5650
20. Zimmermann KC, Sarbia M, Weber AA, Borchard F, Gabbert HE, Schror K: Cyclooxygenase-2 expression in human esophageal carcinoma. Cancer Res 1999, 59:198–204
21. Tucker ON, Dannenberg AJ, Yang EK, Zhang F, Teng L, Daly JM, Soslow RA, Masferrer JL, Woerner BM, Koki AT, Fahey III TJ: Cyclooxygenase-2 expression is up-regulated in human pancreatic cancer. Cancer Res 1999, 59:987–990
22. Chan G, Boyle JO, Yang EK, Zhang F, Sacks PG, Shah JP, Edelstein D, Soslow RA, Koki AT, Woerner BM, Masferrer JL, Dannenberg AJ: Cyclooxygenase-2 expression is up-regulated in squamous cell carcinoma of the head and neck. Cancer Res 1999, 59:991–994
23. Wolff H, Saukkonen K, Anttila S, Karjalainen A, Vainio H, Ristimaki A: Expression of cyclooxygenase-2 in human lung carcinoma. Cancer Res 1998, 58:4997–5001
24. Hida T, Yatabe Y, Achiwa H, Muramatsu H, Kozaki K, Nakamura S, Ogawa M, Mitsudomi T, Sugiura T, Takahashi T: Increased expression of cyclooxygenase 2 occurs frequently in human lung cancers, specifically in adenocarcinomas. Cancer Res 1998, 58:3761–3764
25. Achiwa H, Yatabe Y, Hida T, Kuroishi T, Kozaki K, Nakamura S, Ogawa M, Sugiura T, Mitsudomi T, Takahashi T: Prognostic significance of elevated cyclooxygenase 2 expression in primary, resected lung adenocarcinomas. Clin Cancer Res 1999, 5:1001–1005
26. Hida T, Kozaki K, Muramatsu H, Masuda A, Shimizu S, Mitsudomi T, Sugiura T, Ogawa M, Takahashi T: Cyclooxygenase-2 inhibitor induces apoptosis and enhances cytotoxicity of various anticancer agents in non-small cell lung cancer cell lines. Clin Cancer Res 2000, 6:2006–2011
27. Coffey RJ, Hawkey CJ, Damstrup L, Graves-Deal R, Daniel VC, Dempsey PJ, Chinery R, Kirkland SC, DuBois RN, Jetton TL, Morrow JD: Epidermal growth factor receptor activation induces nuclear targeting of cyclooxygenase-2, basolateral release of prostaglandins, and mitogenesis in polarizing colon cancer cells. Proc Natl Acad Sci USA 1997, 94:657–662
28. Matsuura H, Sakaue M, Subbaramaiah K, Kamitani H, Eling TE, Dannenberg AJ, Tanabe T, Inoue H, Arata J, Jetten AM: Regulation of cyclooxygenase-2 by interferon gamma and transforming growth factor alpha in normal human epidermal keratinocytes and squamous carcinoma cells. Role of mitogen-activated protein kinases. J Biol Chem 1999, 274:29138–29148
29. Ridley SH, Dean JL, Sarsfield SJ, Brook M, Clark AR, Saklatvala J: A

p38 MAP kinase inhibitor regulates stability of interleukin-1-induced cyclooxygenase-2 mRNA. FEBS Lett 1998, 439:75–80
30. Newton R, Stevens DA, Hart LA, Lindsay M, Adcock IM, Barnes PJ: Superinduction of COX-2 mRNA by cycloheximide and interleukin-1beta involves increased transcription and correlates with increased NF-kappaB and JNK activation. FEBS Lett 1997, 418:135–138
31. Chen CC, Sun YT, Chen JJ, Chiu KT: TNF-alpha-induced cyclooxygenase-2 expression in human lung epithelial cells: involvement of the phospholipase C-gamma 2, protein kinase C-alpha, tyrosine kinase, NF-kappa B-inducing kinase, and I-kappa B kinase 1/2 pathway. J Immunol 2000, 165:2719–2728
32. Sheng H, Williams CS, Shao J, Liang P, DuBois RN, Beauchamp RD: Induction of cyclooxygenase-2 by activated Ha-ras oncogene in Rat-1 fibroblasts and the role of mitogen-activated protein kinase pathway. J Biol Chem 1998, 273:22120–22127
33. Subbaramaiah K, Altorki N, Chung WJ, Mestre JR, Sampat A, Dannenberg AJ: Inhibition of cyclooxygenase-2 gene expression by p53. J Biol Chem 1999, 274:10911–10915
34. Moriya Y, Niki T, Yamada T, Matsuno Y, Kondo H, Hirohashi S: Increased expression of laminin-5 and its prognostic significance in small-sized lung adenocarcinoma: an immunohistochemical analysis of 102 cases. Cancer 2001, 91:1129–1141
35. Zhang K, Kramer RH: Laminin 5 deposition promotes keratinocyte motility. Exp Cell Res 1996, 227:309–322
36. Tani T, Lumme A, Linnala A, Kivilaakso E, Kiviluoto T, Burgeson RE, Kangas L, Leivo I, Virtanen I: Pancreatic carcinomas deposit laminin-5, preferably adhere to laminin-5, and migrate on the newly deposited basement membrane. Am J Pathol 1997, 151:1289–1302
37. Kikkawa Y, Umeda M, Miyazaki K: Marked stimulation of cell adhesion and motility by ladsin, a laminin-like scatter factor. J Biochem (Tokyo) 1994, 116:862–869
38. Verrando P, Lissitzky JC, Sarret Y, Winberg JO, Gedde-Dahl Jr T, Schmitt D, Bruckner-Tuderman L: Keratinocytes from junctional epidermolysis bullosa do adhere and migrate on the basement membrane protein nicein through alpha 3 beta 1 integrin. Lab Invest 1994, 71:567–574
39. Pyke C, Romer J, Kallunki P, Lund LR, Ralfkiaer E, Dano K, Tryggvason K: The gamma 2 chain of kalinin/laminin 5 is preferentially expressed in invading malignant cells in human cancers. Am J Pathol 1994, 145:782–791
40. Pyke C, Salo S, Ralfkiaer E, Romer J, Dano K, Tryggvason K: Laminin-5 is a marker of invading cancer cells in some human carcinomas and is coexpressed with the receptor for urokinase plasminogen activator in budding cancer cells in colon adenocarcinomas. Cancer Res 1995, 55:4132–4139
41. Sordat I, Bosman FT, Dorta G, Rousselle P, Aberdam D, Blum AL, Sordat B: Differential expression of laminin-5 subunits and integrin receptors in human colorectal neoplasia. J Pathol 1998, 185:44–52
42. Koshikawa N, Moriyama K, Takamura H, Mizushima H, Nagashima Y, Yanoma S, Miyazaki K: Overexpression of laminin gamma2 chain monomer in invading gastric carcinoma cells. Cancer Res 1999, 59:5596–5601
43. Soini Y, Maatta M, Salo S, Tryggvason K, Autio-Harmainen H: Expression of the laminin gamma 2 chain in pancreatic adenocarcinoma. J Pathol 1996, 180:290–294
44. Skyldberg B, Salo S, Eriksson E, Aspenblad U, Moberger B, Tryggvason K, Auer G: Laminin-5 as a marker of invasiveness in cervical lesions. J Natl Cancer Inst 1999, 91:1882–1887
45. Kosmehl H, Berndt A, Strassburger S, Borsi L, Rousselle P, Mandel U, Hyckel P, Zardi L, Katenkamp D: Distribution of laminin and fibronectin isoforms in oral mucosa and oral squamous cell carcinoma. Br J Cancer 1999, 81:1071–1079
46. Ono Y, Nakanishi Y, Ino Y, Niki T, Yamada T, Yoshimura K, Saikawa M, Nakajima T, Hirohashi S: Clinicopathologic significance of laminin-5 gamma2 chain expression in squamous cell carcinoma of the tongue: immunohistochemical analysis of 67 lesions. Cancer 1999, 85:2315–2321
47. Kainulainen T, Autio-Harmainen H, Oikarinen A, Salo S, Tryggvason K, Salo T: Altered distribution and synthesis of laminin-5 (kalinin) in oral lichen planus, epithelial dysplasias and squamous cell carcinomas. Br J Dermatol 1997, 136:331–336
48. Tomizawa Y, Kohno T, Fujita T, Kiyama M, Saito R, Noguchi M, Matsuno Y, Hirohashi S, Yamaguchi N, Nakajima T, Yokota J: Correlation between the status of the p53 gene and survival in patients with stage I non-small cell lung carcinoma. Oncogene 1999, 18:1007–1014
49. Travis W, Colby T, Corrin B, Shimosato Y, Brambilla E. World Health Organization: Histological Typing of Lung and Pleural Tumours. Berlin, Springer, 1999
50. Sobin L, Wittekind L: TNM classification of malignant tumours. New York, John Wiley & Sons, Inc., 1997
51. Kanai Y, Ushijima S, Nakanishi Y, Hirohashi S: Reduced mRNA expression of the DNA demethylase, MBD2, in human colorectal and stomach cancers. Biochem Biophys Res Commun 1999, 264:962–966
52. Mizushima H, Miyagi Y, Kikkawa Y, Yamanaka N, Yasumitsu H, Misugi K, Miyazaki K: Differential expression of laminin-5/ladsin subunits in human tissues and cancer cell lines and their induction by tumor promoter and growth factors. J Biochem (Tokyo) 1996, 120:1196–1202
53. Ono Y, Nakanishi Y, Gotoh M, Sakamoto M, Hirohashi S: Epidermal growth factor receptor gene amplification is correlated with laminin-5 γ2 chain expression in oral squamous cell carcinoma cell lines. Cancer Lett 2002, 175:197–204
54. Olayioye MA, Neve RM, Lane HA, Hynes NE: The ErbB signaling network: receptor heterodimerization in development and cancer. EMBO J 2000, 19:3159–3167
55. Sen R, Baltimore D: Multiple nuclear factors interact with the immunoglobulin enhancer sequences. Cell 1986, 46:705–716
56. Rayet B, Gelinas C: Aberrant rel/nfkb genes and activity in human cancer. Oncogene 1999, 18:6938–6947
57. Novak U, Cocks BG, Hamilton JA: A labile repressor acts through the NFkappaB-like binding sites of the human urokinase gene. Nucleic Acids Res 1991, 19:3389–3393
58. Huang S, Robinson JB, Deguzman A, Bucana CD, Fidler IJ: Blockade of nuclear factor-kappaB signaling inhibits angiogenesis and tumorigenicity of human ovarian cancer cells by suppressing expression of vascular endothelial growth factor and interleukin 8. Cancer Res 2000, 60:5334–5339
59. Kunsch C, Rosen CA: NF-kappa B subunit-specific regulation of the interleukin-8 promoter. Mol Cell Biol 1993, 13:6137–6146
60. Jones MK, Wang H, Peskar BM, Levin E, Itani RM, Sarfeh IJ, Tarnawski AS: Inhibition of angiogenesis by anti-inflammatory drugs: insight into mechanisms and implications for cancer growth and ulcer healing. Nat Med 1999, 5:1418–1423
61. Attiga FA, Fernandez PM, Weeraratna AT, Manyak MJ, Patierno SR: Inhibitors of prostaglandin synthesis inhibit human prostate tumor cell invasiveness and reduce the release of matrix metalloproteinases. Cancer Res 2000, 60:4629–4637
62. Rozic JG, Chakraborty C, Lala PK: Cyclooxygenase inhibitors retard murine mammary tumor progression by educing tumor cell migration, invasiveness and angiogenesis. Int J Cancer 2001, 93:497–506
63. Dohadwala M, Luo J, Zhu L, Lin Y, Dougherty GJ, Sharma S, Huang M, Pold M, Batra RK, Dubinett SM: Non-small cell lung cancer cyclooxygenase-2-dependent invasion is mediated by CD44. J Biol Chem 2001, 276:20809–20812
64. Dormond O, Foletti A, Paroz C, Ruegg C: NSAIDS inhibit αVβ3 integrin-mediated and cdc42/Rac-dependent endothelial-cell spreading, migration and angiogenesis. Nat Med 2001, 7:1041–1047
65. Giannelli G, Falk-Marzillier J, Schiraldi O, Stetler-Stevenson WG, Quaranta V: Induction of cell migration by matrix metalloproteinase-2 cleavage of laminin-5. Science 1997, 277:225–228
66. Goldfinger LE, Stack MS, Jones JCR: Processing of laminin-5 and its functional consequences: role of plasmin and tissue-type plasminogen activator. J Cell Biol 1998, 141:255–265
67. Koshikawa N, Giannelli G, Cirulli V, Miyazaki K, Quararnta V: Role of cell surface metalloprotease MT1-MMP in epithelial cell migration over laminin-5. J Cell Biol 2000, 148:615–624
68. Peller S: Clinical implications of p53: effect on prognosis, tumor progression and chemotherapy response. Semin Cancer Biol 1998, 8:379–387
69. Mukhopadhyay D, Tsiokas L, Sukhatme VP: Wild-type p53 and v-Src exert opposing influences on human vascular endothelial growth factor gene expression. Cancer Res 1995, 55:6161–6165
70. Forrester K, Ambs S, Lupold SE, Kapust RB, Spillare EA, Weinberg WC, Felley-Bosco E, Wang XW, Geller DA, Tzeng E, Billiar TR, Harris CC: Nitric oxide-induced p53 accumulation and regulation of inducible nitric oxide synthase expression by wild-type p53. Proc Natl Acad Sci USA 1996, 93:2442–2447
71. Santhanam U, Ray A, Sehgal PB: Repression of the interleukin 6 gene promoter by p53 and the retinoblastoma susceptibility gene product. Proc Natl Acad Sci USA 1991, 88:7605–7609

ACADEMIC PRESS

Biochemical and Biophysical Research Communications 297 (2002) 1058–1061

BBRC

www.academicpress.com

G-CSF stimulates angiogenesis and promotes tumor growth: potential contribution of bone marrow-derived endothelial progenitor cells

Takeshi Natori,[a] Masataka Sata,[b,*] Miwa Washida,[b] Yasunobu Hirata,[b] Ryozo Nagai,[b] and Masatoshi Makuuchi[a]

[a] *Department of Surgery, University of Tokyo, Graduate School of Medicine, Tokyo 113-8655, Japan*
[b] *Department of Cardiovascular Medicine, University of Tokyo, Graduate School of Medicine, 7-3-1 Hongo, Bunkyo-ku, Tokyo 113-8655, Japan*

Received 20 August 2002

Abstract

Solid tumors require neovascularization for their growth. Recent evidence indicates that bone marrow-derived endothelial progenitor cells (EPCs) contribute to tumor angiogenesis. We show here that granulocyte colony-stimulating factor (G-CSF) markedly promotes growth of the colon cancer inoculated into the subcutaneous space of mice, whereas G-CSF had no effect on cancer cell proliferation in vitro. The accelerated tumor growth was associated with enhancement of neovascularization in the tumor. We found that bone marrow-derived cells participated in new blood vessel formation in tumor. Our findings suggest that G-CSF may have potential to promote tumor growth, at least in part, by stimulating angiogenesis in which bone marrow-derived EPCs play a role.

Solid tumors require blood supply and then must recruit new blood vessels for their growth [1]. It is generally accepted that tumor growth is 'angiogenesis'-dependent, and hence, blocking 'angiogenesis' could be a strategy to arrest tumor growth [2].

Vessel development consists of two different processes, vasculogenesis and angiogenesis [3]. Vasculogenesis is the in situ differentiation of mesodermal precursors to angioblasts that differentiate into endothelial cells (ECs) to form the primitive capillary network. Angiogenesis is the sprouting of new capillaries from preexisting blood vessels. Until recently, vasculogenesis was considered limited to early embryogenesis. Postnatal neovascularization was thought to result from angiogenesis [4]. However, recent studies identified circulating endothelial progenitor cells (EPCs), suggesting that undifferentiated precursors mobilized from the bone marrow substantially contribute to postnatal vessel formation [5]. Granulocyte-colony stimulating factor (G-CSF) is one of a family of glycoprotein molecules, which stimulates the production of white blood cells, particularly granulocytes [6]. G-CSF also mobilizes hematopoietic stem cells into peripheral blood [7]. It was reported that granulocyte-macrophage colony-stimulating factor (GM-CSF) mobilizes EPCs into peripheral circulation and promotes angiogenesis in ischemic tissues [8].

In this study, we investigated the effects of G-CSF on tumor growth and angiogenesis in vivo. Results suggest that G-CSF may have potential to promote cancer development through its ability to stimulate tumor-associated angiogenesis, in which bone marrow-derived EPCs play a role.

Materials and methods

Study protocol. All protocols involving experimental animals were in accordance with the institutional guidelines for animal care of the University of Tokyo. Male eight-week-old C57BL/6 mice were purchased from SLC Japan (Shizuoka, Japan). Either saline or human recombinant G-CSF (20 μg/kg/day) was administered intraperitoneally

* Corresponding author. Fax: +81-3-3814-0021.
E-mail address: msata-circ@umin.ac.jp (M. Sata).

0006-291X/02/$ - see front matter © 2002 Elsevier Science (USA). All rights reserved.
PII: S0006-291X(02)02335-5

everyday starting 5 days before tumor inoculation. The mice were anesthetized with pentobarbital (50 mg/kg, intraperitoneally). We suspended 2×10^7 murine syngeneic colon cancer cells (CMT93, American Type Culture Collection, Rockville, MD) in 0.1 ml ECM gel (Sigma, St. Louis, MO) and injected them subcutaneously into the left flank fold of C57BL/6J mice. We measured tumor size by calipers everyday. Tumor volume was estimated as width^2 × length × 0.52. Mice were euthanized at 21 days after implantation. The tumors were excised, fixed in methanol, and embedded in paraffin. ROSA26 mice that express LacZ ubiquitously were originally purchased from Jackson Laboratory (Bar Harbor, ME). Bone marrow transplantation was performed as described [9].

Measurement of capillary density. Sections (5 μm) were de-paraffinized and incubated with a rat monoclonal antibody against murine CD31 (clone MEC13.1, BD PharMingen, San Diego, CA) [10]. Antibody distribution was visualized using the avidin–biotin-complex technique and Vector Red Chromogenic substrate (Vector Laboratories, Burlingame, CA), followed by counterstaining with hematoxylin. Capillaries were identified by positive staining for CD31 and morphology. Ten different fields from each tissue preparation were randomly selected and capillaries were counted. Capillary density was expressed as the number of capillaries per square millimeter.

Detection of bone marrow-derived endothelial cells in cancer. Tumors were embedded in OCT compound and snap frozen in liquid nitrogen. Frozen sections (5 μm) were fixed in formalin and stained with anti-LacZ rabbit polyclonal antibody (ICN, Aurora, OH) or anti-CD31 rat monoclonal antibody, followed by incubation with FITC-conjugated anti-rabbit Ig and rhodamine-conjugated anti-rat Ig secondary antibodies. Nuclei were counterstained with Hoechst 33258. The sections were observed under a confocal microscope (FLUOVIEW FV300, Olympus, Tokyo).

Cell proliferation assay in vivo. CMT93 cells were maintained in Dulbecco's modified Eagle's medium supplemented with 10% fetal bovine serum. The 7×10^4 cells were cultured in a well of 24-well culture plate/ml in the absence or presence of G-CSF for 24 h. Cells were counted after trypsinization.

Statistical analysis. All results are expressed as means ± SEM. Means were statistically compared by ANOVA followed by Student's t test. A value of $p < 0.05$ was considered to be significant.

Results

Promotion of tumor growth by G-CSF

To determine the effect of G-CSF on tumor growth, we used a tumor implantation model. We injected 2×10^7 murine syngeneic colon cancer cells (CMT93) subcutaneously into the left flank fold of C57BL/6 mice. The mice were treated with either G-CSF (20 μg/kg/day, $n = 4$) or saline ($n = 4$). Tumor growth in the G-CSF-treated group markedly exceeded that in the saline-treated group ($p < 0.01$) (Fig. 1).

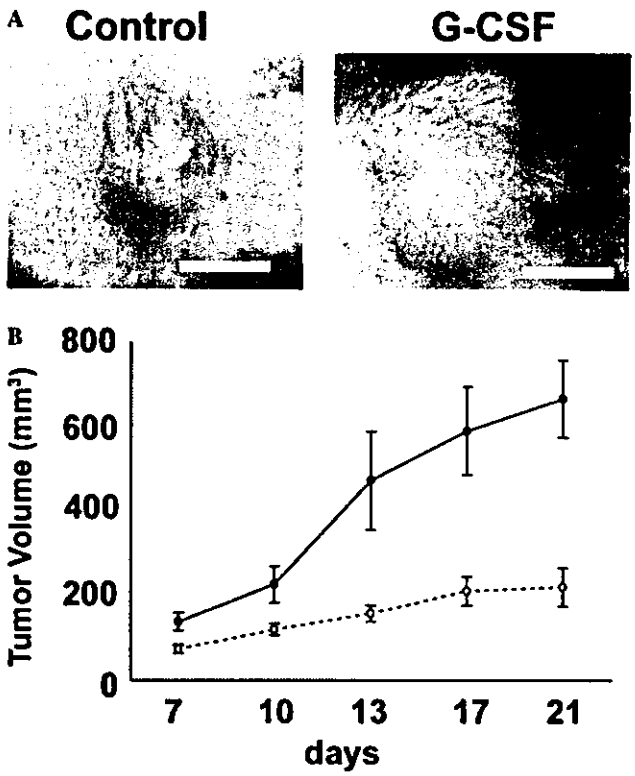

Fig. 1. Effect of G-CSF on tumor growth in vivo. (A) We implanted 2×10^7 murine syngeneic colon cancer cells (CMT93) subcutaneously into the left flank fold of C57BL/6 mice. Mice received 20 μg/kg/day of G-CSF (closed circle, $n = 6$) or saline (open circle, $n = 6$) starting 5 days before implantation. Scale bar, 1 cm. (B) Tumor size was measured by calipers. Tumor volume was estimated as width 2 × length × 0.52.

Effect of G-CSF on tumor cell proliferation in vitro

Next, we investigated whether G-CSF directly stimulates proliferation of carcinoma cells. The 7×10^4 CMT93 cells were cultured in the absence or presence of G-CSF (10^{-14}–10^{-6} M) for 24 h. We found that G-CSF had no effect on cell proliferation in vitro (Fig. 2).

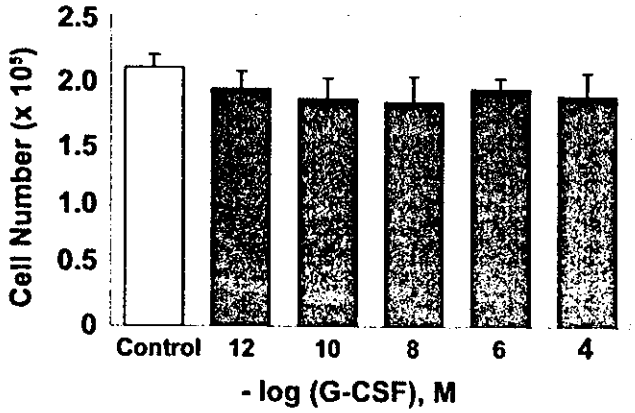

Fig. 2. Effect of G-CSF on carcinoma cell proliferation in vitro. The 7×10^4 CMT93 cells were cultured in the absence or presence of G-CSF at the indicated concentration. After 24 h, the cells were counted.

Effects of G-CSF on neovascularization in tumors

To study the effect of G-CSF on neovascularization in tumors, we harvested the tumors at 21 days after implantation. Anti-CD31 immunostaining revealed that

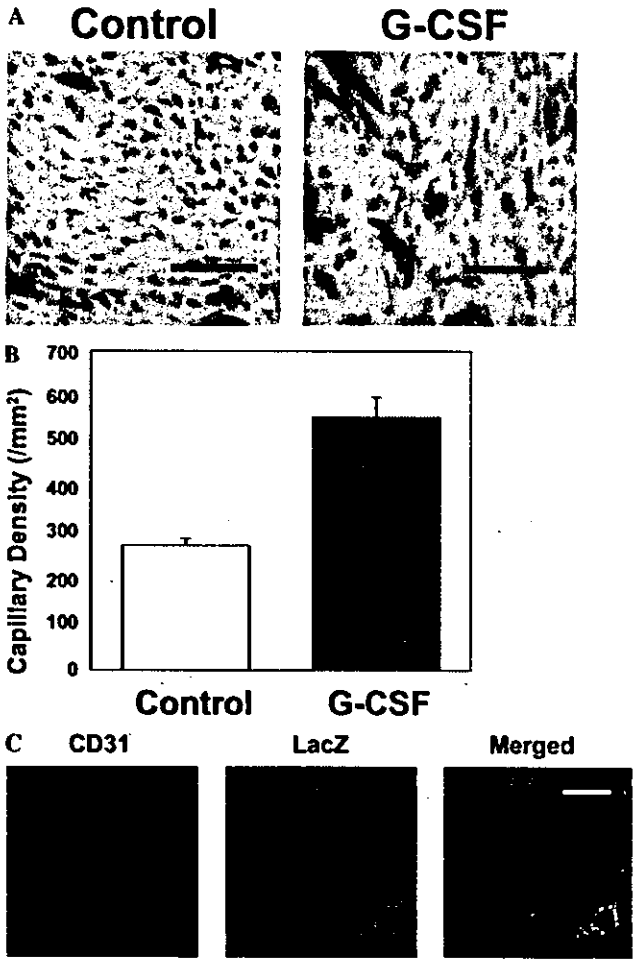

Fig. 3. Effects of G-CSF on neovascularization in tumor. (A) Cross-sections were stained for CD31. Scale bar, 50 μm. (B) Capillary density was measured. (C) The 1×10^7 CMT93 cells were implanted in the wild-type mice whose bone marrow had been reconstituted with that of ROSA26 mice. Mice received G-CSF. At day 7, tumors were collected for immunofluorescence double staining to detect CD31 (red) and LacZ (green). Bar, 20 μm.

many new vessels had been formed in tumor (Fig. 3A). We found that the capillary density in the G-CSF-treated group was significantly higher than that in the vehicle-treated mice (554 ± 44 versus 273 ± 15 capillaries/mm^2, $p < 0.01$) (Fig. 3B). To study potential contribution of bone marrow cells to new capillary formation in tumor, we inoculated carcinoma cells in the wild-type mice whose bone marrow had been replaced with that of ROSA26 mice. The mice were treated with G-CSF (20 μg/kg/day) for 7 days. Immunofluorescence study revealed that some CD31-positive endothelial cells in tumor were derived from bone marrow cells expressing LacZ (Fig. 3C).

Discussion

In this study, we found that G-CSF promoted tumor growth and neovascularization in vivo, whereas G-CSF had no effect on cancer cell proliferation in vitro. The accelerated tumor growth by G-CSF was associated with enhanced new vessel formation. To our knowledge, this is the first report that G-CSF promotes tumor growth and neovascularization in vivo, while previous studies showed that G- and GM-CSF induce endothelial cells to proliferate and stimulate wound healing [11,12].

G-CSF is known to mobilize CD34-positive cells into peripheral blood. Recent studies have demonstrated that circulating CD34$^+$/Flk-1$^+$ cells can differentiate into endothelial cells [13,14] and that G-CSF-mobilized CD34$^+$ cells augment neovascularization [15]. In this study, we also found that G-CSF enhanced neovascularization in which bone marrow cells participated. It may be plausible that G-CSF influenced differentiation and mobilization of EPCs that were incorporated into the new vessels.

There is increasing interest in potential use of G-CSF to regenerate various cell types from bone marrow cells (BMCs). It was reported that BMCs can differentiate de novo into cardiac myocytes [16]. G-CSF therapy is expected to increase the number of circulating stem cells derived from BMCs, which may participate in myocardial repair of infarcted heart [16]. Since our findings suggest that G-CSF may potentially promote cancer growth, we should carefully rule out the existence of latent cancer before administration of G-CSF in patients. Similarly, we should be careful when we administer G-CSF to treat neutropenia after chemotherapy [17], because G-CSF might enhance progression of residual cancer.

In summary, our results suggest that G-CSF promotes tumor growth, at lease in part, by stimulating neovascularization. Our findings have implication for clinical use of G-CSF in patients.

Acknowledgments

This study was supported in part by grants from the Ministry of Health, Labor and Welfare of Japan and the Motor Vehicle Trust Fund for Research of Heart Diseases (Dr. Sata).

References

[1] J. Folkman, What is the evidence that tumors are angiogenesis dependent?, J. Natl. Cancer Inst. 82 (1990) 4–6.
[2] J. Folkman, Tumor angiogenesis: therapeutic implications, N. Engl. J. Med. 285 (1971) 1182–1186.
[3] P. Carmeliet, Mechanisms of angiogenesis and arteriogenesis, Nat. Med. 6 (2000) 389–395.
[4] J. Folkman, Y. Shing, Angiogenesis, J. Biol. Chem. 267 (1992) 10931–10934.
[5] M. Peichev, A.J. Naiyer, D. Pereira, Z. Zhu, W.J. Lane, M. Williams, M.C. Oz, D.J. Hicklin, L. Witte, M.A. Moore, S. Rafii, Expression of VEGFR-2 and AC133 by circulating human CD34(+) cells identifies a population of functional endothelial precursors, Blood 95 (2000) 952–958.

[6] S.C. Clark, R. Kamen, The human hematopoietic colony-stimulating factors, Science 236 (1987) 1229–1237.
[7] J. Tanaka, T. Miyake, T. Shimizu, T. Wakayama, M. Tsumori, K. Koshimura, Y. Murakami, Y. Kato, Effect of continuous subcutaneous administration of a low dose of G-CSF on stem cell mobilization in healthy donors: a feasibility study, Int. J. Hematol. 75 (2002) 489–492.
[8] T. Takahashi, C. Kalka, H. Masuda, D. Chen, M. Silver, M. Kearney, M. Magner, J.M. Isner, T. Asahara, Ischemia- and cytokine-induced mobilization of bone marrow-derived endothelial progenitor cells for neovascularization, Nat. Med. 5 (1999) 434–438.
[9] M. Sata, A. Saiura, A. Kunisato, A. Tojo, S. Okada, T. Tokuhisa, H. Hirai, M. Makuuchi, Y. Hirata, R. Nagai, Hematopoietic stem cells differentiate into vascular cells that participate in the pathogenesis of atherosclerosis, Nat. Med. 8 (2002) 403–409.
[10] M. Sata, H. Nishimatsu, E. Suzuki, S. Sugiura, M. Yoshizumi, Y. Ouchi, Y. Hirata, R. Nagai, Endothelial nitric oxide synthase is essential for the HMG-CoA reductase inhibitor cerivastatin to promote collateral growth in response to ischemia, FASEB J. 15 (2001) 2530–2532.
[11] F. Bussolino, J.M. Wang, P. Defilippi, F. Turrini, F. Sanavio, C.J. Edgell, M. Aglietta, P. Arese, A. Mantovani, Granulocyte- and granulocyte-macrophage-colony stimulating factors induce human endothelial cells to migrate and proliferate, Nature 337 (1989) 471–473.
[12] F. Bussolino, M. Ziche, J.M. Wang, D. Alessi, L. Morbidelli, O. Cremona, A. Bosia, P.C. Marchisio, A. Mantovani, In vitro and in vivo activation of endothelial cells by colony-stimulating factors, J. Clin. Invest. 87 (1991) 986–995.
[13] T. Asahara, T. Murohara, A. Sullivan, M. Silver, R. van der Zee, T. Li, B. Witzenbichler, G. Schatteman, J.M. Isner, Isolation of putative progenitor endothelial cells for angiogenesis, Science 275 (1997) 964–967.
[14] Q. Shi, S. Rafii, M.H. Wu, E.S. Wijelath, C. Yu, A. Ishida, Y. Fujita, S. Kothari, R. Mohle, L.R. Sauvage, M.A. Moore, R.F. Storb, W.P. Hammond, Evidence for circulating bone marrow-derived endothelial cells, Blood 92 (1998) 362–367.
[15] A.A. Kocher, M.D. Schuster, M.J. Szabolcs, S. Takuma, D. Burkhoff, J. Wang, S. Homma, N.M. Edwards, S. Itescu, Neovascularization of ischemic myocardium by human bone-marrow-derived angioblasts prevents cardiomyocyte apoptosis, reduces remodeling and improves cardiac function, Nat. Med. 7 (2001) 430–436.
[16] D. Orlic, J. Kajstura, S. Chimenti, D.M. Bodine, A. Leri, P. Anversa, Transplanted adult bone marrow cells repair myocardial infarcts in mice, Ann. N. Y. Acad. Sci. 938 (2001) 221–229.
[17] G.J. Lieschke, A.W. Burgess, Granulocyte colony-stimulating factor and granulocyte-macrophage colony-stimulating factor, N. Engl. J. Med. 327 (1992) 28–35.

Int. J. Cancer: 103, 455–465 (2003)

Publication of the International Union Against Cancer

GLYPICAN-3, OVEREXPRESSED IN HEPATOCELLULAR CARCINOMA, MODULATES FGF2 AND BMP-7 SIGNALING

Yutaka MIDORIKAWA[1,2], Shumpei ISHIKAWA[1], Hiroko IWANARI[3], Takeshi IMAMURA[4], Hirohiko SAKAMOTO[5], Kohei MIYAZONO[4], Tatsuhiko KODAMA[6], Masatoshi MAKUUCHI[2], and Hiroyuki ABURATANI[1]*

[1]*Genome Science Division, Research Center for Advanced Science and Technology, University of Tokyo, Tokyo, Japan*
[2]*Hepato-Biliary-Pancreatic Surgery Division, Department of Surgery, University of Tokyo, Tokyo, Japan*
[3]*Institute of Immunology, Tokyo, Japan*
[4]*Department of Biochemistry, The Cancer Institute, Tokyo, Japan*
[5]*Department of Surgery, Saitama Cancer Center, Tokyo, Japan*
[6]*Molecular Biology and Medicine, Research Center for Advanced Science and Technology, University of Tokyo, Tokyo, Japan*

The Glypican (GPC) family is a prototypical member of the cell-surface heparan sulfate proteoglycans (HSPGs). The HSPGs have been demonstrated to interact with growth factors, act as coreceptors and modulate growth factor activity. Here we show that based on oligonucleotide array analysis, GPC3 was upregulated in hepatocellular carcinoma (HCC). By northern blot analysis, GPC3 mRNA was found to be upregulated in 29 of 52 cases of HCC (55.7%). By Western blot analysis carried out with a monoclonal anti-GPC3 antibody we generated, the GPC3 protein was found to be overexpressed in 6 hepatoma cell lines, HepG2, Hep3B, HT17, HuH6, HuH7 and PLC/PRF/5, as well as 22 tumors (42.3%). To investigate the role of overexpressed GPC3 in liver cancer, we analyzed its effects on cell growth of hepatoblastoma-derived cells. Overexpression of GPC3 modulated cell proliferation by inhibiting fibroblast growth factor 2 (FGF2) and bone morphogenetic protein 7 (BMP-7) activity. An interaction of GPC3 and FGF2 was revealed by co-immunoprecipitation, while GPC3 was found to inhibit BMP-7 signaling through the Smad pathway by reporter gene assay. The modulation of growth factors by GPC3 may help explain its role in liver carcinogenesis. In addition, the ability of HCC cells to express GPC3 at high levels may serve as a new tumor marker for HCC.

Key words: *heparan sulfate proteoglycan; hepatocarcinogenesis; heparin-binding growth factors; tumor marker; cell proliferation*

Glypican 3 (GPC3) is a member of the heparan sulfate proteoglycans (HSPGs) and binds to the cell membrane via glycosilphosphatidylinositol anchors.[1] HSPGs are well known to interact with growth factors through heparan sulfate (HS) chains, to act as a coreceptor for heparin binding growth factors and ultimately, to stimulate or inhibit growth factor activity.[2–4] HSPGs have been recently identified to act as coreceptors for fibroblast growth factor 2 (FGF2), to promote it to bind its receptor and finally, to play an important role in the FGF2 signaling pathway.[5–9]

On the other hand, bone morphogenetic protein (BMP), a secreted growth factor and a subset of transforming growth factor-β (TGF-β) superfamily, regulates cell proliferation and apoptosis during morphogenesis of bone, renal and neuronal tissues.[3] Among the BMP family members, BMP-7 is known to control collecting tubule cell proliferation and apoptosis in a dose-dependent manner[10] and GPC3 is reported to modulate BMP-mediated effects during renal branching morphogenesis using GPC3-/mouse.[4]

Clinically, it has been reported that the GPC3 gene is mutated in Simpson-Golabi-Behmel syndrome, an X-linked disorder characterized by pre- and postnatal overgrowth.[11] GPC3 is also reported to be able to interact with insulin-like growth factor 2 (IGF2), mediated by the HS chains and an altered regulation of IGF2,[11] although the binding of GPC3 to IGF2 is still controversial.[12] Such evidence suggest that GPC3 could well be involved in the control of cell proliferation and/or the induction of apoptosis, as indicated by certain experimental studies.[13,14]

In cancer tissues, the levels of transcriptionally expressed GPC3 are variable, although overexpression of the protein has yet to be conclusively demonstrated. In ovarian cancer, it is reported that GPC3 is expressed in the normal ovary, but that silencing of this gene takes place in a significant proportion of ovarian cancer cell lines as a result of hypermethylation of the GPC3 promoter. Therefore, GPC3 has come to be understood to be a suppressor gene in the ovary.[14] Downregulation of GPC3 in mesothelioma indeed has been reported, whereas GPC3 is highly expressed in normal mesothelial cells.[15] Accordingly, the function of GPC3 in the ovary, like that in the mesothelium, is thought to either induce apoptosis or control cell proliferation.

In contrast, GPC3 mRNA has also been demonstrated to be highly expressed in embryonal tumors,[16] colon cancer[17] and hepatocellular carcinoma (HCC)[18,19] in comparison with the corresponding normal tissues. However, an upregulation of GPC3 in cancerous tissues is contradictory to the commonly understood function of this molecule and, therefore, the function of GPC3 has been hypothesized to be varied in a tissue-specific manner, that is, GPC3 induces apoptosis in breast or ovary, but acts as oncofetal protein in liver and colon.[13]

In our study, it was found that the GPC3 mRNA is highly expressed in HCC, as shown by gene expression profile analysis and validated by Northern blot. To confirm overexpression of GPC3 protein, we generated a monoclonal anti-GPC3 antibody and performed immunohistochemistry and Western blot analysis. To determine the role of GPC3 in hepatocarcinogenesis, we established a liver cancer cell line, in which GPC3 expression can be induced by tetracycline withdrawal. We show here that GPC3 interacts with FGF2, inhibits the BMP-7 signaling pathway and modulates the activity of FGF2 and BMP-7. All of these findings suggest that GPC3 does not only regulate cell proliferation under certain conditions but that it also plays an important role in hepatocarcinogenesis.

Grant sponsor: The Ministry of Education, Science, Sports and Culture of Japan (H.A.). Grant numbers: Grants-in-Aid for Scientific Research (B) 12557051 and 13218019 and Scientific Research on Priority Areas (C) 12217031. Grant sponsor: Uehara Memorial Foundation; Grant sponsor: Sagawa Foundation for Promotion of Cancer Research.

*Correspondence to: Genome Science Division, Research Center for Advanced Science and Technology, The University of Tokyo, 4-6-1 Komaba, Meguro-ku, Tokyo 153-8904, Japan. Fax: +81-3-5452-5355. E-mail: haburata-tky@umin.ac.jp

Received 2 April 2002; Revised 12 August 2002; Accepted 21 September 2002

DOI 10.1002/ijc.10856

MATERIAL AND METHODS

Tissue samples

Forty-five patients with HCC who had undergone hepatectomy at either the Hepato-Biliary-Pancreatic Surgery Division, Department of Surgery, Graduate School of Medicine, University of Tokyo, or at the Department of Surgery, Saitama Cancer Center, were included in our study after obtaining informed consent. According to the definition of multicentric HCCs proposed by Tsuda *et al.*,[20] 5 patients were diagnosed as having 2 multicentric nodules and 1 patient 3 nodules; therefore, 52 tumors and 45 noncancerous liver tissues were taken. As controls, normal liver tissues were obtained from 8 patients with metastatic liver cancer. The average of 45 patients including 30 male and 15 female was 64.4 ± 7.7 years. Serum test showed 11 patients were positive for hepatitis B surface antigen and 34 for hepatitis C virus antibody. Histologic findings demonstrated that of 52 tumors, 22 were well-differentiated hepatocellular carcinoma (WD), 21 moderately differentiated hepatocellular carcinoma (MD) and 9 poorly differentiated hepatocellular carcinoma (PD), whereas the background liver of 13 patients were chronic hepatitis (CH) and 32 liver cirrhosis (LC).

Six tumors were accompanied with vascular invasion and the average of tumor size was 28.0 ± 13.7 mm in diameter. The surgical specimens were immediately cut into small pieces after resection, snap-frozen in liquid nitrogen and stored in a −80°C freezer.

Cell lines and culture conditions

The hepatoblastoma cell line HepG2 was obtained from the American Type Culture Collection. HCC cell lines Hep3B, HT17 and Li-7 were kindly provided by Cell Resource Center for Biomedical Research, Tohoku University (Miyagi, Japan). The HCC cell lines HLE, HuH7 and PLC/PRF/5 and the hepatoblastoma cell line HuH6 were purchased from Health Science Research Resource Bank (Osaka, Japan). HepG2, Hep3B, HLE, HuH6 and PLC/PRF/5 were maintained in DMEM (Sigma, St Louis, MO), HT17 was maintained in MEM (Sigma) and HuH7 and Li7 in RPMI 1640 (Sigma). Tetracycline-regulated HepG2 cells (HY-Toff) were a gift from Dr. Ying Huang (University of Tokyo).[21]

Vector construction and transfection

cDNA synthesized from colon cancer cell line, Caco2, which has no abnormality of GPC3 sequence, was used as a template for RT-PCR using Advantage II (Clontech, Palo Alto, CA). After confirmation of GPC3 coding with an API Prism 3100 Genetic Analyzer (Applied Biosystems, Foster City, CA), GPC3 cDNA

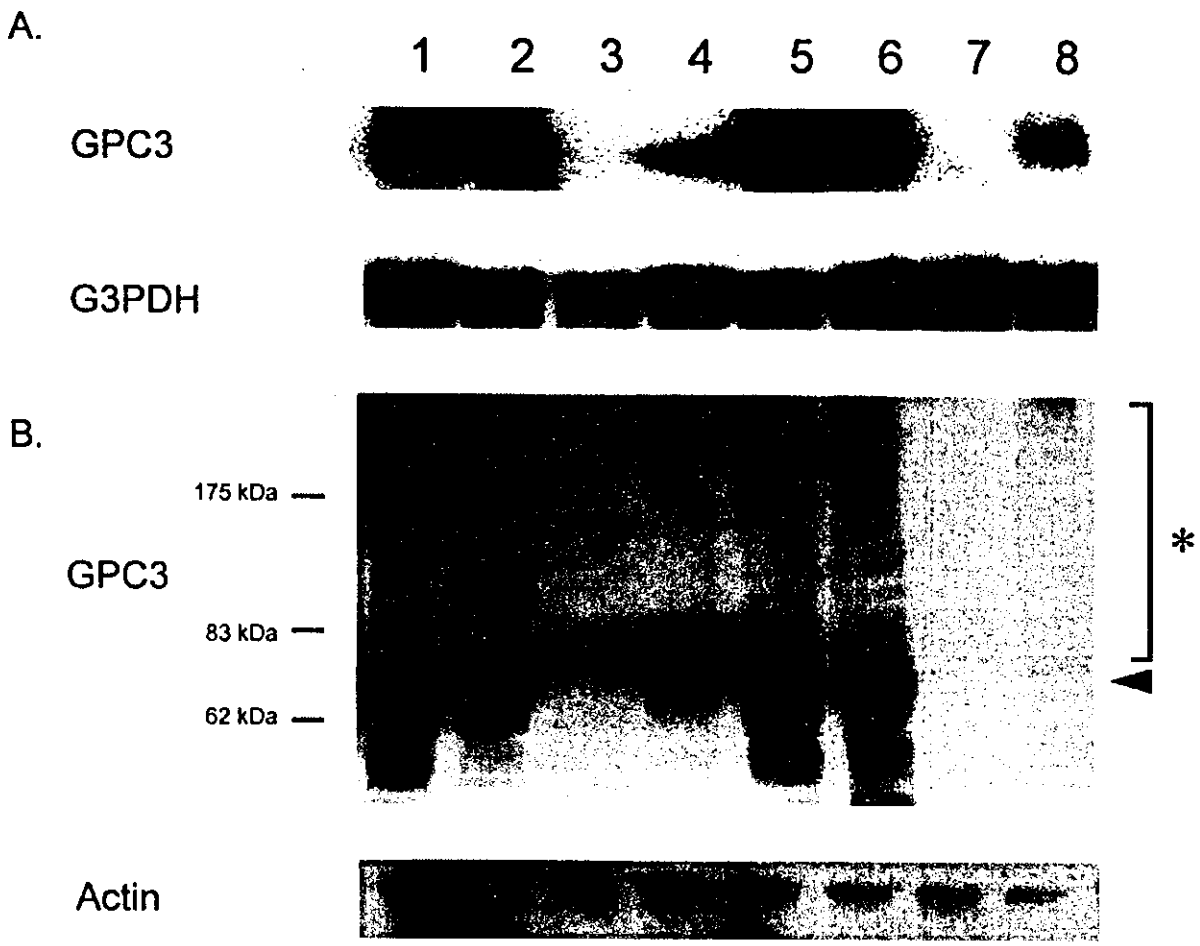

FIGURE 1 – Expression of GPC3 mRNA and protein in hepatoma cell lines. *(a)* Northern blot analysis of the GPC3 expression levels in hepatoma cell lines. Lane 1, HepG2; lane 2, Hep3B; lane 3, HLE; lane 4, HT17; lane 5, HuH6; lane 6, HuH7; lane 7, Li-7; lane 8, PLC/PRF/5. *(b)* Western blot analysis of the GPC3 expression levels in hepatoma cell lines. Arrowhead, core protein of GPC3; asterisk, glycosylated protein. Numbers on the left represent molecular mass markers.

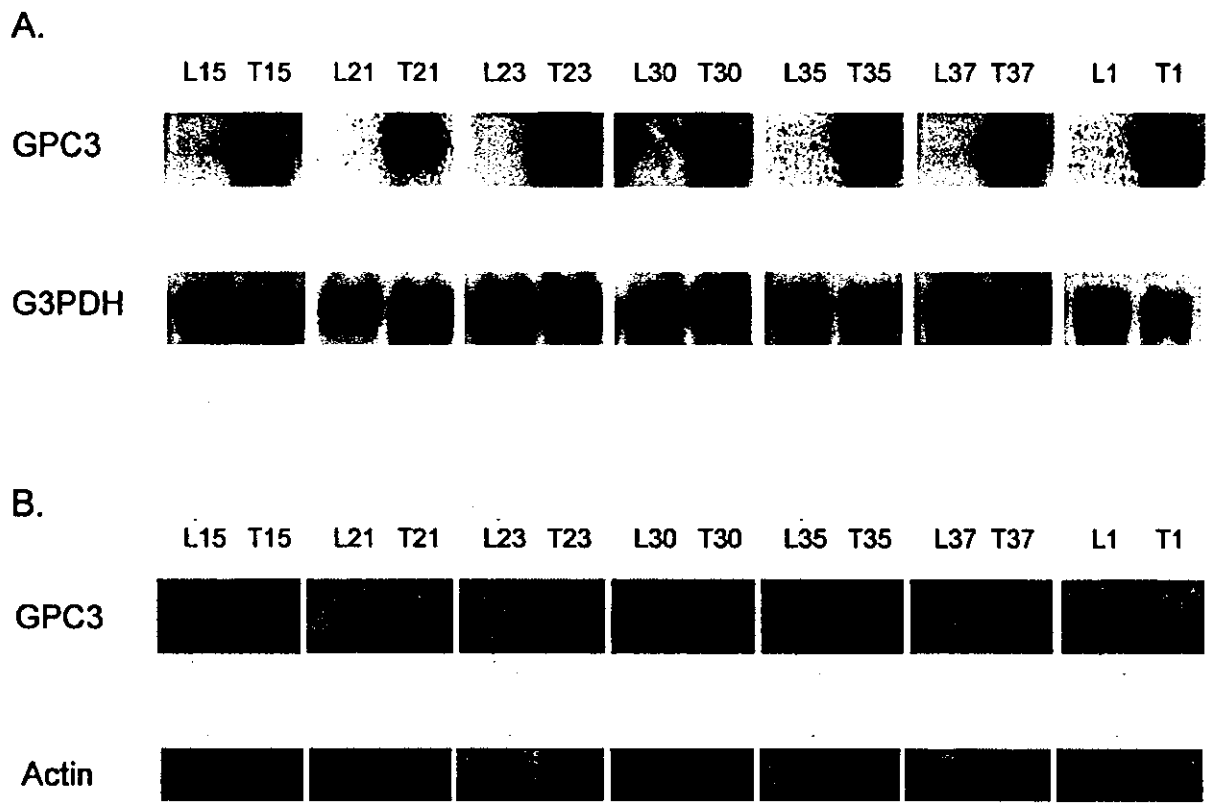

FIGURE 2 – Expression of GCP3 in hepatocellular carcinoma and noncancerous tissues. *(a)* Northern blot analysis of the GPC3 expression levels in paired noncancerous tissues (L) and HCC (T). The number on the top of the figure refers to the patient's no., shown in Table I. *(b)* Western blot analysis of the GPC3 expression levels of paired noncancerous tissues (L) and HCC (T).

was subcloned into the pBI-EGFP vector (Clontech) and termed pBI-EGFP-GPC3. The primers used for the GPC3 preparation contained an *Eco*RV and *Nhe*I site, respectively, attached to the 5′ end, a sense primer, 5′-GATATC-ATGGCCGGGACCGTGCG-CACCGCGT and an antisense primer, 5′-GCTAGC-TCAGTG-CACCAGGAAGAAGAAGCAC. To generate a HY-Toff cell line with tetracycline-inducible GPC3 expression, HY-Toff cells were cotransfected with both pBI-EGFP-GPC3 and pBabepuro using a Tfx-20 (Promega, Madison, WI), followed by selection in culture medium containing 2 μg/ml puromycin (Nacalai tesque, Kyoto, Japan) and 5 ng/ml Doxycycline hydrochloride (Dox) (Sigma). Surviving clones were isolated, expanded and dubbed HY-Toff-GPC3 clones. To induce GPC3 expression, cells were incubated without Dox in serum-containing medium.

RNA extraction and Northern blot analysis

Total RNA was isolated from frozen tissue with an ISOGENE™ kit (Nippon Gene, Tokyo, Japan), according to the manufacturer's protocol. The Northern blot analysis, using 10 μg total RNA, was performed as described.[22] ^{32}P-radiolabeled cDNA probes were prepared with a Strip-EZ DNA kit (Ambion, Austin, TX) using a human GPC3 cDNA as templates.

Generation of monoclonal antibody against GPC3

A peptide composed of 17 amino acid residues, from 355 to 371 of GPC3, was chemically synthesized (Peptide Institute, Osaka, Japan). Female BALB/c mice (6 weeks of age) were immunized 3 times every 2 weeks with the synthetic peptide GPC3 conjugated with the Keyhole Lmpet Hemocyanin (KLH; Calbiochem, San Diego, CA). Spleen cells were isolated 3 days after the last immunization and fused with NS-1 myeloma cells (Dainippon Pharmaceutical, Osaka, Japan) by a conventional method.[23] Hybridomas were selected by the enzyme-linked immunosorbent assay (ELISA) with the synthetic peptide in each well of a 96-well titer plate (Corning, Acton, MA). Peroxidase-conjugated anti-mouse IgG antibody (ICN Pharmaceuticals, Costa Mesa, OH) was used as the second antibody. Absorbence at 450 nm was measured following incubation with TMB Soluble Reagent (ScyTek, Logan, UT). Positive hybridomas were cloned by limited dilution. The large-scale production of monoclonal antibodies was carried out by growing the hybridoma cells in mouse ascites. The immunoglobulin was purified by ammonium sulfate precipitation.

Protein extraction, Western blot and immunohistochemical analysis

Cells and tissue samples were lysed in a lysis buffer [20mM HEPES (pH 7.5), 150 mM NaCl, 1 mM EDTA, 10 μg/ml, 1 mM PMSF, 1.0% Triton X-100, 0.5% deoxycholate, 0.1% SDS] after collection from a 100 mm dish and disruption, respectively. Proteins (20 μg) were resolved on 7.5% SDS-PAGE and transferred to Hybond-P membranes (Amersham Pharmacia, Piscataway, NJ). Western blot analysis was performed using anti-GPC3 antibody, with anti-actin (Santa Cruz, Santa Cruz, CA) as control. After incubation with horseradish peroxidase-conjugated antibody sheep anti-mouse IgG (Amersham Pharmacia), labeled proteins were detected with an ECL-Plus detection system (Amersham Pharmacia).

For the detection of GPC3 on the cell surface of HCC cells, noncancerous and cancerous tissues with or without GPC3 expression as determined by Western blot analysis were subjected to

TABLE I - CLINICAL DATA AND PATHOLOGIC FINDINGS ACCORDING TO GPC3 EXPRESSION

Patient no.	Age	Gender	HVI	BGL	Diff. grade	VI	Tumor Size (mm)	NB (HCC)	NB (Liver)	WB (HCC)	WB (Liver)
1	48	M	HB	LC	WD	−	22	++	−	−	+
2	69	M	HC	LC	WD	−	15	+	−	−	−
3	72	F	HC	CH	WD	−	33	−	−	−	−
4	69	F	HC	LC	WD	−	40	−	−	−	−
5	62	M	HB	CH	WD	−	31	−	−	−	−
6	64	M	HC	LC	WD	−	15	−	−	−	−
7	59	F	HC	LC	WD	−	20	−	−	−	−
8	70	M	HC	LC	WD	−	16	−	−	−	−
9	75	M	HC	CH	WD	−	40	−	−	−	−
10	67	M	HC	LC	WD	−	17	−	−	−	−
11	62	M	HC	CH	WD	−	25	−	−	−	−
12	66	M	HC	CH	WD	+	36	−	−	−	−
13	67	M	HC	LC	WD	−	26	−	−	−	−
14	68	M	HC	LC	WD	−	22	−	−	−	−
15	66	M	HC	LC	WD	−	23	+++	−	++	−
16	62	F	HC	LC	WD	−	15	+	−	−	−
17	71	M	HB	LC	WD	−	22	+	−	+	−
18	65	M	HC	LC	MD	−	21	−	−	−	+
19	69	F	HB	LC	MD	−	38	−	−	−	−
20	60	M	HC	LC	MD	−	65	−	−	+	+
21	47	M	HB	CH	MD	+	24	+++	−	++	−
22	71	F	HC	LC	MD	−	22	++	−	++	−
23	71	F	HC	LC	MD	−	30	+++	−	+++	−
24	69	M	HC	CH	MD	−	50	−	−	−	−
25	70	F	HC	LC	MD	−	23	+++	−	+++	−
26	53	M	HB	LC	MD	−	45	−	−	−	−
27	63	F	HC	CH	MD	−	20	+++	−	+++	−
28	50	M	HB	LC	MD	+	25	++	−	+	+
29	49	M	HB	LC	MD	+	22	++	−	+++	−
30	61	F	HC	LC	MD	−	41	+++	+	++	−
31	48	M	HB	LC	MD	−	35	+	−	−	−
32	78	M	HC	LC	PD	−	43	−	−	−	−
33	54	M	HB	CH	PD	−	11	++	−	+	+
34	68	F	HC	CH	PD	−	23	−	−	−	−
35	56	F	HB	CH	PD	−	42	+++	−	+++	−
36	73	F	HC	LC	PD	−	24	−	+	−	−
37	70	F	HC	LC	PD	+	30	+++	−	++	−
38	63	M	HC	LC	PD	−	35	++	+	++	−
39	72	M	HC	CH	PD	−	89	++	−	+++	−
40	71	M	HC	LC	WD	−	13	−	−	−	−
					MD	−	15	+++		++	
41	63	M	HC	LC	WD	−	20	+	−	−	−
					MD	−	20	++		−	
42	66	F	HC	LC	WD	−	40	++	−	+	−
					MD	−	27	++		++	
43	70	M	HC	LC	WD	−	13	+	−	−	−
					PD	+	22	++		++	
44	70	M	HC	LC	MD	−	25	−	−	−	−
					MD	−	20	++		+	
45	65	M	HC	CH	WD	−	20	++	+	−	−
					MD	−	25	+		−	
					MD	−	22	−		−	

HVI, hepatitis viral infection; BGL, background liver; VI, vascular invasion; NB, Northern blot analysis; WB, Western blot analysis; M, male; F, female. −, GPC3 negative; +, weakly positive; ++, moderately positive; +++, strongly positive in NB and WB. Patient nos. 1–39 have 1 tumor; nos. 40–44, 2 tumors; no. 45 3 tumors.

immunohistochemistry using an LSAB system. After 5 μm-thick frozen sections on glass slides were fixed by ethanol and treated using proteinase K, sections were stained with anti-GPC3 antibody by means of an LSAB kit/HRP (Dako, Glostrup, Denmark A/S) according to the manufacturer's protocol.

Cell growth assay

Cell growth assay was performed in the same manner as described previously.[24] Briefly, 3 independent HY-Toff-GPC3 clones were plated overnight at a density of 10,000 cells/well in 96-well plates, washed with PBS and subsequently incubated in 100 μl DMEM with 1% FBS in the presence or absence of Dox in order to control GPC3 expression. Growth factors, IGF2, FGF2, BMP-7, TGF-β3 or HB-EGF (R&D Systems, Minneapolis, MN), were added at various concentrations. Forty-eight hours after incubation, cells were counted with an MTT Cell Growth Kit (Chemicon International, Temecula, CA) and compared in triplicate in each clone.

Purification of FGF2 and GPC3 protein complex

Human FGF2 coding cDNA was obtained by the same method described above, using the sense primer, 5′-GAATTC-ATGGC AGCCGGGAGCATCACCA and the antisense primer, 5′-CTC-GAG-TCAGCTCTTAGCAGACATTGG, designed to amplify the FGF2 coding sequence, including the *Eco*RI and *Xho*I sites at the 5′ and 3′ end, respectively. By means of the *Eco*RI and *Xho*I sites, the FGF2 PCR product was incorporated into the pcDNA4 vector (Invitrogen, Carlsbad, CA), and this construct was named pcDNA-FGF2. HY-Toff-GPC3 cells were transiently transfected with pcDNA-FGF2. Cells were incubated without Dox for 48 hr and

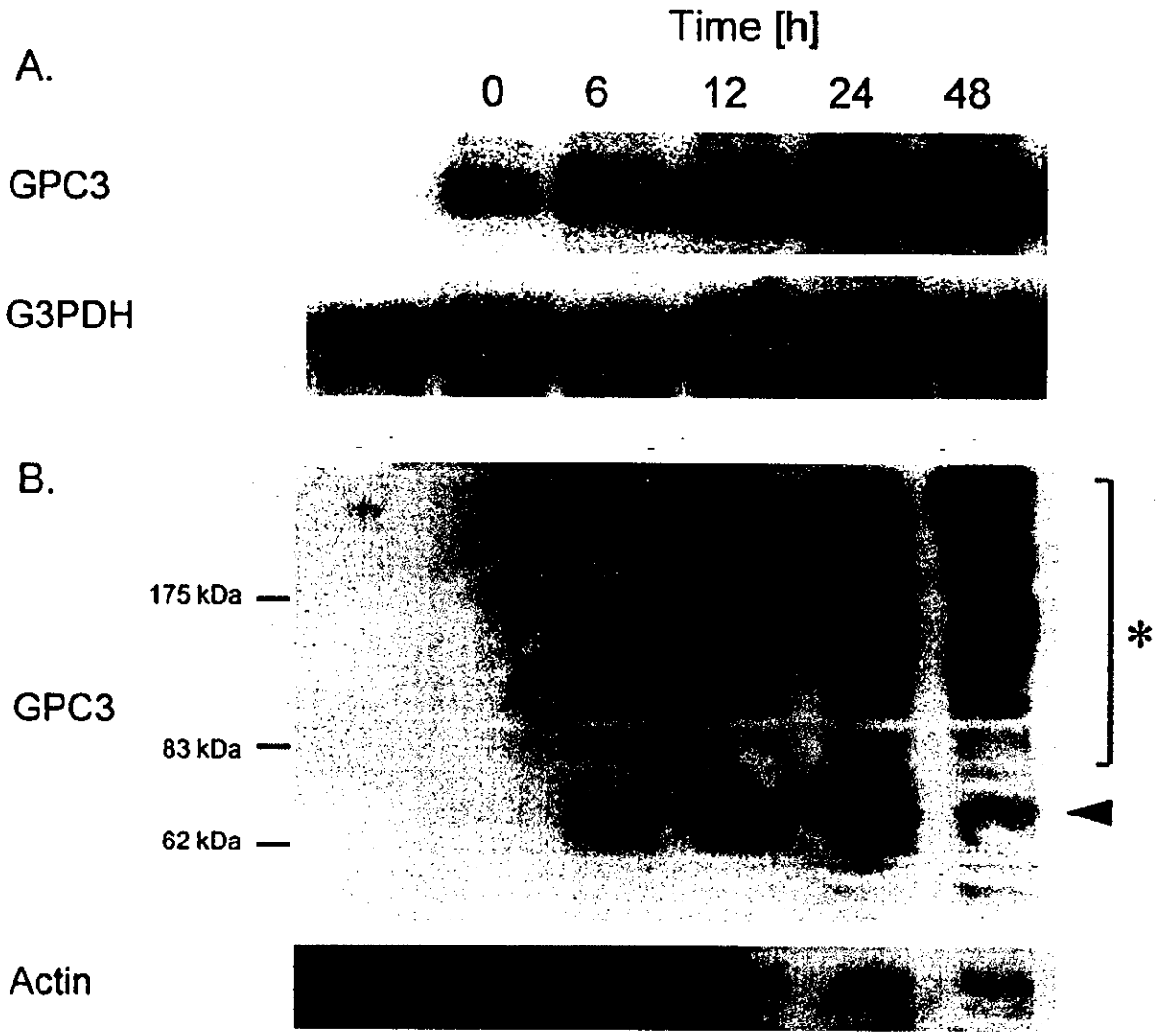

FIGURE 3 – Regulation of GPC3 expression in HY-Toff-GPC3 cells. *(a)* Northern blot analysis of the GPC3 expression level after induction by removal of Dox. The mRNA GPC3 levels elevate time-dependently, and leaky GPC3 expression was detected in the cells even without induction. The number at the top of the figure means the time after removal of Dox. Left lane, HY-Toff cells. *(b)* Western blot analysis by monoclonal anti-GPC3 antibody of the GPC3 expression levels after induction by removal of Dox. Arrowhead, core protein of GPC3; asterisk, glycosylated protein. The expression of GPC3 can be seen to increase in accordance with the GPC3 mRNA.

lysed in a lysis buffer [20 mM HEPES (pH 7.5), 150 mM NaCl, 1 mM EDTA, 10 μg/ml, 1 mM PMSF].

Interaction of GPC3 and FGF2 *in vivo* was assessed by immunoprecipitation assay. To isolate GPC3-binding FGF2 and FGF2-binding GPC3, whole-cell extracts were incubated with anti-GPC3 antibody or anti-FGF2 antibody-binding (Santa Cruz) Protein G sepharose (Amersham Pharmacia) for 1 hr with gentle rotation. After being washed with lysis buffer, the resin was boiled at 90°C with the SDS sample buffer. The supernatant was subjected to Western blot analysis to allow estimation of the interaction of FGF2 and GPC3.

Luciferase assay

The plasmid 3GC2-Lux is a luciferase reporter construct containing 3 repeats of a GC-rich sequence derived from the BMP-responsive element in the Smad6 promoter.[25] Briefly, a fragment of the mouse Smad6 gene promoter, including the BMP-responsive element was inserted into pGL2-Basic, and transcriptional activation activity was determined by luciferase assay in the presence or absence of Doxycycline using HY-Toff cells. HY-Toff cells were cotransfected with 3GC2-Lux and pRL-TK (Promega) with Tfx-20 in 6-well plates. Forty-eight hours after transfection, cells were plated at a density of 10,000 cells/well in 96-well plates with or without Dox, and BMP-7 added at various concentrations. Luciferase assay was performed using FireLite (Packard BioScience, Groningen, the Netherlands), according to the manufacturer's protocol, and luciferase activity was measured by TopCount (Packard BioScience).

Statistical analysis

The values of continuous variables are presented as the mean ± SD. The statistical analysis of the parameters collected from the 2

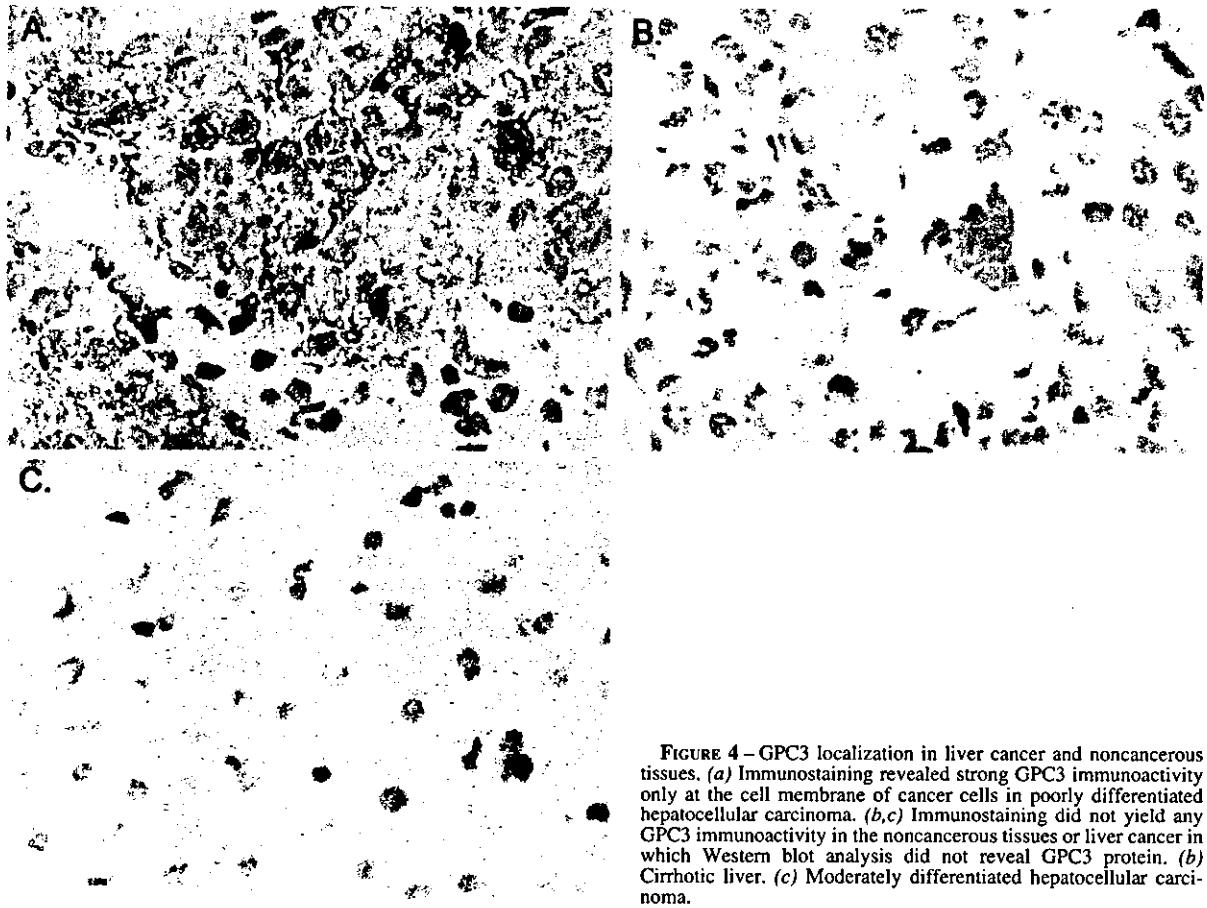

FIGURE 4 – GPC3 localization in liver cancer and noncancerous tissues. *(a)* Immunostaining revealed strong GPC3 immunoactivity only at the cell membrane of cancer cells in poorly differentiated hepatocellular carcinoma. *(b,c)* Immunostaining did not yield any GPC3 immunoactivity in the noncancerous tissues or liver cancer in which Western blot analysis did not reveal GPC3 protein. *(b)* Cirrhotic liver. *(c)* Moderately differentiated hepatocellular carcinoma.

groups, *i.e.*, the GPC3-positive and -negative groups on Western blot analysis, was determined by the χ^2 test and Student's *t*-test. Two values of the cell growth assays were compared using a 2-way factorial ANOVA test. Statistical differences were considered significant at $p < 0.05$.

RESULTS

Transcriptional expression of GPC3 by northern blot analysis

Northern blot analysis was performed on 8 liver cancer cell lines and all the tissue samples. Among the cell lines, the 2.3-kb GPC3 mRNA transcript was detected in HepG2, Hep3B, HuH6 and HuH7 at a high level and HT17, PLC/PRF/5 at a low level (Fig. 1*a*). Of the 52 tumor samples taken from 45 patients, 22 exhibited moderate to high levels of GPC3 mRNA, whereas 7 tumor samples exhibited low levels, and the intensity of the expression of GPC3 in all of these cases was higher than that in the noncancerous tissues (Fig. 2*a*). According to differentiation grade, 9 tumors exhibited the 2.3 kb GPC3 mRNA in 22 WDs (40.9%), 14 in 21 MDs (66.7%) and 6 in 9 PDs (66.7%), respectively. On the other hand, in noncancerous tissues the GPC3 mRNA was below the level of detection in all of the NL samples and was detected at a low level in 1 CH and 3 LCs (Fig. 2*a*). Therefore, the positive rates of GPC3 mRNA in HCC and chronic liver disease were 55.7% and 8.8%, respectively. Between the 2 groups, GPC3 transcript-positive or -negative of the tumor, there were no significant differences in any clinical data.

Validation of monoclonal antibody of GPC3

To confirm that the GPC3 cDNA had been cloned into the HY-Toff cells, Northern blotting was carried out with a GPC3 probe. We found that although HepG2 cells highly express endogeneous GPC3 mRNA, in the course of establishment of HY-Toff cells, these cells have lost the expression of GPC3 and the clone that does not express GPC3 has been selected (Fig. 2*a*). Zero, 6, 12, 24 and 48 hr after removing Dox, GPC3 mRNA was detectable, with the intensity dependent on the time elapsed since induction (Fig. 3*a*).

Using HY-Toff and HY-Toff-GPC3 cells, we performed Western blot analysis with an anti-GPC3 monoclonal antibody (Fig. 3*b*). Neither the 65 kDa core protein nor glycosylated protein were detected in the HY-Toff or HY-Toff-GPC3 cells with Dox, whereas a 65 kDa band did manifest in HY-Toff-GPC3 cells after the removal of Dox. The intensity of the glycosylated GPC3 protein became stronger in accordance with time after the removal of Dox, as had been the case in Northern blot analysis.

To investigate the localization of GPC3, immunohistochemical analysis with an anti-GPC3 antibody was performed on the frozen specimens (Fig. 4). Cancerous tissues in which a 65 kDa protein was detected by Western blot analysis exhibited a strong immunoactivity on the cell membrane but not in the cytoplasm or nuclei (Fig. 4*a*). In contrast, HCC without GPC3 expression on Western blot analysis and in the noncancerous tissues did not exhibit any GPC3 immunoactivity (Fig. 4*b,c*).

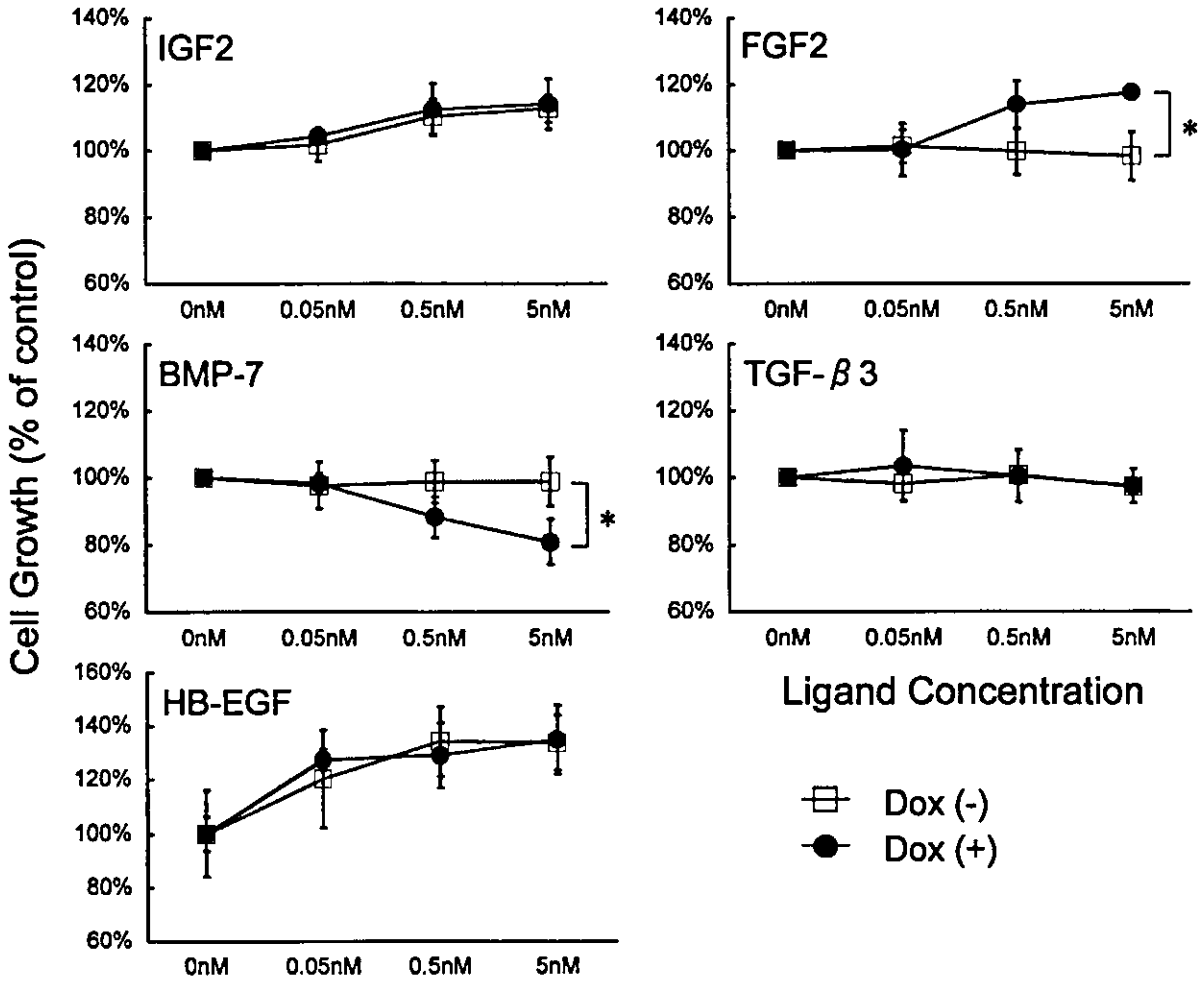

FIGURE 5 – The effects of overexpressed GPC3 on growth factor responsiveness. To keep GPC3 expression suppressed, 5 ng/ml Dox was added to the medium, and upon the removal of Dox, the expression of GPC3 was induced. HY-Toff-GPC3 cells were incubated with (filled circles) or without (open squares) Dox at the indicated concentrations of IGF2, FGF2, BMP-7, TGF-β3 and HB-EGF. Data are expressed as the percentage of change from unstimulated controls and are the mean ± SD of 3 determinations per experiment from 3 separate experiments ($*p < 0.05$).

Expression of GPC3 protein by Western blot analysis

To validate whether the GPC3-translated protein is really up-regulated in HCC, Western blot analysis was performed with the 8 HCC cell lines and all the tissue samples. Western blot analysis with an anti-GPC3 monoclonal antibody demonstrated a 65 kDa protein in 6 cell lines, HepG2, Hep3B, HT17, HuH6, HuH7 and PLC/PRF/5, and the intensity of expression was in accordance with the results of the Northern blot analysis (Fig. 1*b*). In 52 HCC cases, 15 tumors exhibited moderate to high levels of the 65 kDa band and 7 low levels (42.3%) (Fig. 2*b*). According to differentiation grade, 4 tumors exhibited the 65 kDa protein in 22 WDs (18.1%), 12 in 21 MDs (57.1%) and 6 in 9 PDs (66.7%), respectively.

On the other hand, in the noncancerous tissues, a 65 kDa band was not observed in any of the NL tissues but was detected in 1 sample of CH and 3 samples of LC at low levels (8.8%). However, in all of the noncancerous samples in which the GPC3 protein was detected by Western blot analysis, the 2.3 kb GPC3 transcript also was not detectable by Northern blot analysis (Fig. 2*b*).

To clarify the factors responsible for the positive rate of GPC3 translation, we carried out a statistical analysis that examined a variety of clinicopathologic factors including the patients' background, histologic findings in tumors and noncancerous tissues, tumor size and liver functions between the 2 groups. We found that there was only a significant difference in terms of the differentiation grade of the tumor in GPC3 protein.

Effects of GPC3 on growth factor-induced cell proliferation in HepG2 cells

First, to investigate whether enhanced expression of GPC3 can either stimulate or suppress cell growth, GPC3 was overexpressed in HY-Toff cells. However, it could not be shown that GPC3 is able to control cell proliferation in a period of up to 48 hr (data not shown). Accordingly, to determine whether enhanced expression of GPC3 regulates growth factor action, HY-Toff cells were incubated in the presence or absence of the stimulatory growth factors IGF2 or FGF2, the inhibitory growth factors BMP-7 or TGF-β and heparin-binding growth factor HB-EGF (Fig. 5). Although there was no difference in the presence or absence of overexpressed